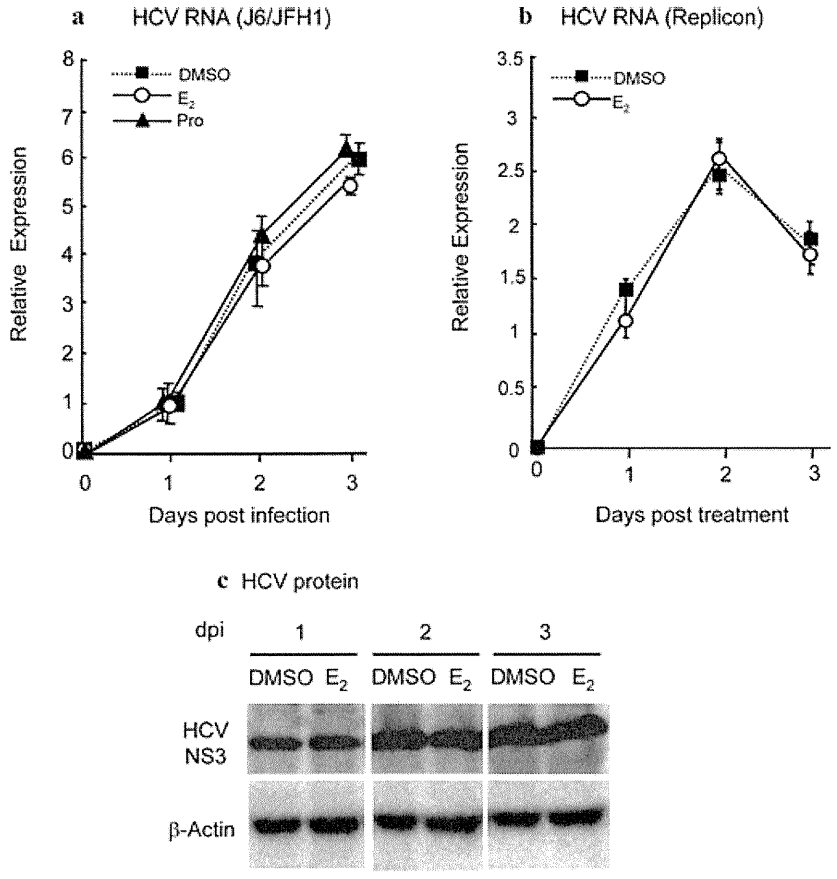

Fig. 2. Effects of E_2 and P_4 on HCV RNA replication and HCV protein synthesis. (a) HCV RNA replication. Huh-7.5 cells were inoculated with HCV at a multiplicity of infection of 1.0, incubated for 2 hr, and cultured for 0, 1, 2 and 3 days after virus infection. The HCV-infected cells were treated with E_2 (0.4 μM) or DMSO (control) from 2 hr to sampling time (days 1, 2 and 3). HCV RNA replication levels were determined by real-time quantitative RT-PCR and normalized with β-actin mRNA levels. Data are shown as mean ± SEM. (b) Huh-7.5 cells harboring a full-genomic HCV RNA replicon (23) were treated with E_2 (0.4 μM) or DMSO, and HCV RNA replication levels determined as in (a). (c) HCV protein synthesis. HCV-infected cells were treated with E2 or DMSO as in (a) and the amount of HCV protein synthesis determined by immunoblot analysis using anti-NS3 antibody. The degree of β-actin expression as determined by anti-β-actin antibody served as a control. dpi, days postinfection.

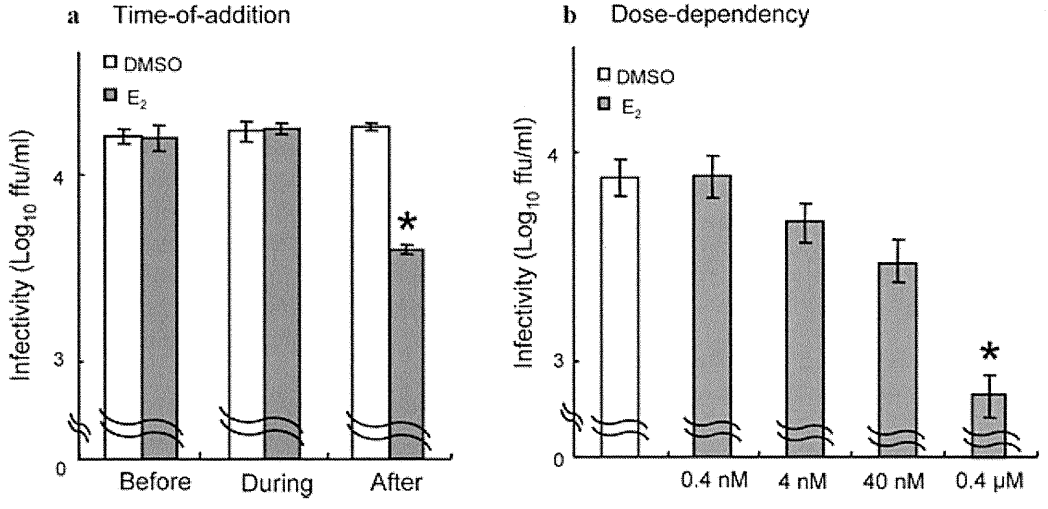

Fig. 3. Kinetic analysis of E_2–mediated inhibition of HCV virion production. (a) Time-of-addition experiment. Huh-7.5 cells were inoculated with HCV at a multiplicity of infection of 1.0, incubated for 2 hr, and cultured up to 2 days after virus infection. Treatment of the cells with E_2 (0.4 μM) was performed before or during virus inoculation for 2 hr, or after virus inoculation until sampling time (day 2). The culture supernatants of HCV-infected cells were assayed for viral infectivity. Data are shown as mean ± SEM. *$P < 0.05$, compared with DMSO control. (b) Dose–dependency experiment. Huh-7.5 cells were inoculated with HCV as in (a). The HCV-infected cells were treated with various concentrations of E_2 (0.4 nM to 0.4 μM]) from 2 hr postinfection to sampling time (day 2). The culture supernatants of HCV-infected cells were assayed for viral infectivity. Data are shown as mean ± SEM. *$P < 0.05$, compared with DMSO control.

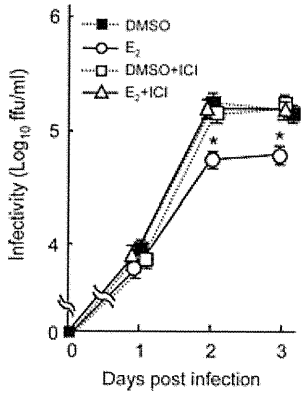

Fig. 4. Effects of ER antagonist, ICI182780, on HCV virion production. Huh-7.5 cells were inoculated with HCV at a multiplicity of infection of 1.0, incubated for 2 hr, and cultured for 0, 1, 2 and 3 days after virus infection. The HCV-infected cells were treated with E_2 (0.4 μM) and/or ICI182780 (1 μM) or DMSO (control) from 2 hr postinfection to sampling time (days 1, 2 and 3). The culture supernatants of HCV-infected cells were assayed for virus infectivity. Data are shown as mean ± SEM. *$P < 0.05$, compared with DMSO control.

Estrogen receptor-α-selective agonist 4, 4′, 4″- (4-propyl-[1H]-pyrazole-1, 3, 5-triyl) trisphenol inhibits HCV virion production

To determine which estrogen receptor(s) is/are involved in the E_2–mediated down-regulation of HCV virion production, we used receptor-specific agonists, such as PPT (an ERα-selective agonist) (20), DPN (an ERβ-selective agonist) (21) and G-1 (a GPR30-selective agonist) (22). Treatment of cells with PPT (10 μM), but not with DPN (10 μM) or G-1 (1 μM), significantly inhibited HCV virion production (Fig. 5). PPT treatment at a concentration of 1 μM also brought about a weak, but significant, inhibition of HCV virion production at 2 days postinfection. On the other hand, PPT did not mediate significant cytotoxicity at the concentrations tested (data not shown).

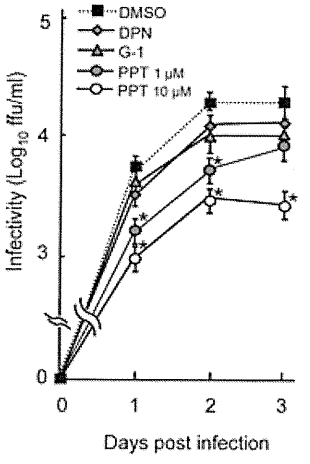

Fig. 5. Effects of ER-specific agonists on HCV virion production. Huh-7.5 cells were inoculated with HCV at a multiplicity of infection of 1.0, incubated for 2 hr, and cultured for 0, 1, 2 and 3 days after virus infection. The HCV-infected cells were treated with PPT (ERα-selective agonist; 1 and 10 μM), DPN (ERβ-selective agonist; 10 μM) or G-1 (GPR30-selective agonist; 1 μM) from 2 hr postinfection to sampling time (days 1, 2 and 3). The culture supernatants of HCV-infected cells were assayed for viral infectivity. Data are shown as mean ± SEM. *$P < 0.05$, compared with DMSO control.

DISCUSSION

We have demonstrated in the present study that treatment of Huh-7.5 cells with E_2 inhibits HCV virion production, but not HCV RNA replication or HCV protein synthesis (Figs 1 and 2). Treatment of the cells with E_2 either prior to, or during, virus inoculation did not significantly suppress HCV virion production (Fig. 3a). These results collectively suggest that E_2 inhibits HCV infection at the virion assembly/secretion level, but not at the level of virus attachment/entry, virus RNA replication or virus protein synthesis. E_2 has been reported to possess antioxidant and anti-apoptotic activities in fibrotic liver and cultured hepatocytes (24, 25). It should be noted, however, that E_2 did not exert anti-apoptotic or cytotoxic (pro-apoptotic) effect under our experimental conditions (Fig. 1b). In contrast to E_2, another female hormone, P_4, did not significantly affect HCV virion production (Fig. 1a).

E_2-mediated inhibition of HCV virion production was abolished by a nuclear ER (ERα and ERβ) antagonist, ICI182780 (Fig. 4), this result suggesting that suppression of HCV virion production may be induced by ER signal transduction. Three types of ER have been reported so far; ERα, ERβ and GPR30 (11–15). To determine which ER is involved in the suppression of HCV virion production, we used ER-specific agonists, PPT (for ERα) (20), DPN (for ERβ) (21) and G-1 (for GPR30) (22). We found that PPT, but not DPN or G-1, inhibits the production of HCV infectious particles (Fig. 5), suggesting that ERα plays an important role in the inhibition of HCV virion production. It has been reported that, in hepatocytes, ERα constitutes a minor proportion of the total ER, and that an estrogen-mediated anti-apoptotic effect is mediated principally through ERβ (26). However, the importance of ERα–mediated signal transduction should not be ignored. The rationale for this assertion is that ERα is known to be involved in lipid metabolism (27), that certain lipid metabolism disorder(s) possibly result(s) in abnormal accumulation of lipid droplets, and that such an accumulation is required for HCV virion maturation in virus-infected cells (27), that certain lipid metabolism disorder(s) possibly result(s) in abnormal accumulation of

lipid droplets, and that such an accumulation is required for HCV virion maturation in virus-infected cells (28). Also, we should not yet exclude the possible importance of ERβ and GPR30, because they may not be expressed at a sufficient level in the Huh7.5 cell line maintained in our laboratory.

Other relevant observations are that ERα interacts with HCV NS5B, the viral RNA polymerase, and promotes association of NS5B with the replication complex in human hepatoma-derived Huh-7 cells, and that tamoxifen, a competitive inhibitor of estrogens, suppresses the ERα–mediated association of NS5B with the replication complex, thereby inhibiting HCV RNA replication (29). Similarly, E_2 binding to ERα may abrogate its interaction with NS5B. However, in our experiments we did not observe E_2–mediated inhibition of HCV RNA replication (Fig. 2a,b). We therefore assume that E_2 inhibits HCV virion production through a mechanism other than E_2–ERα–NS5B interactions. Further study is needed to elucidate this issue.

In conclusion, the most potent physiological estrogen, E_2, inhibits production of HCV infectious particles in Huh-7.5 cell cultures in an ERα–dependent manner. This may explain, at least in part, why the incidence of HCV-associated liver disease is lower in premenopausal women than in postmenopausal women and men.

ACKNOWLEDGMENTS

The authors are grateful to Dr. C. M. Rice for providing Huh7.5 cells and pFL-J6/JFH1. Thanks are also due to Dr. T. Adachi for his technical advice. This study was supported in part by Health and Labor Sciences Research Grants from the Ministry of Health, Labor and Welfare, Japan, and the Japan Science and Technology/Japan International Cooperation Agencies' Science and Technology Research Partnership for Sustainable Development. This study was also carried out as part of the Japan Initiative for Global Research Network on Infectious Diseases, Ministry of Education, Culture, Sports, Science and Technology, Japan, and the Global Center of Excellence Program at Kobe University Graduate School of Medicine.

REFERENCES

1. Shepard C.W., Finelli L., Alter M.J. (2005) Global epidemiology of hepatitis C virus infection. *Lancet Infect Dis* **5:** 558–67.
2. Alberti A., Benvegnù L., Boccato S., Ferrari A., Sebastiani G. (2004) Natural history of initially mild chronic hepatitis C. *Dig Liver Dis* **36:** 646–54.
3. Davis G.L., Alter M.J., El-Serag H., Poynard T., Jennings L.W. (2010) Aging of hepatitis C virus (HCV)-infected persons in the United States: a multiple cohort model of HCV prevalence and disease progression. *Gastroenterology* **138:** 513–21.
4. Armstrong G.L., Wasley A., Simard E.P., McQuillan G.M., Kuhnert W.L., Alter M.J. (2006) The prevalence of hepatitis C virus infection in the United States, 1999 through 2002. *Ann Intern Med* **144:** 705–14.
5. Poynard T., Ratziu V., Charlotte F., Goodman Z., McHutchison J., Albrecht J. (2001) Rates and risk factors of liver fibrosis progression in patients with chronic hepatitis C. *J Hepatol* **34:** 730–9.
6. Massard J., Ratziu V., Thabut D., Moussalli J., Lebray P., Benhamou Y., Poynard T. (2006) Natural history and predictors of disease severity in chronic hepatitis C. *J Hepatol* **44:** S19–24.
7. Di Martino V., Lebray P., Myers R.P., Pannier E., Paradis V., Charlotte F., Moussalli J., Thabut D., Buffet C., Poynard T. (2004) Progression of liver fibrosis in women infected with hepatitis C: long-term benefit of estrogen exposure. *Hepatology* **40:** 1426–33.
8. Shimizu I., Yasuda M., Mizobuchi Y., Ma Y.R., Liu F., Shiba M., Horie T., Ito S. (1998) Suppressive effect of oestradiol on chemical hepatocarcinogenesis in rats. *Gut* **42:** 112–9.
9. Yasuda M., Shimizu I., Shiba M., Ito S. (1999) Suppressive effects of estradiol on dimethylnitrosamine-induced fibrosis of the liver in rats. *Hepatology* **29:** 719–27.
10. Wang C.C., Krantz E., Klarquist J., Krows M., McBride L., Scott E.P., Shaw-Stiffel T., Weston S.J., Thiede H., Wald A., Rosen H.R. (2007) Acute hepatitis C in a contemporary US cohort: modes of acquisition and factors influencing viral clearance. *J Infect Dis* **196:** 1474–82.
11. Hall J.M., Couse J.F., Korach K.S. (2001) The multifaceted mechanisms of estradiol and estrogen receptor signaling. *J Biol Chem* **276:** 36,869–72.
12. Gustafsson J.A. (2003) What pharmacologists can learn from recent advances in estrogen signaling. *Trends Pharmacol Sci* **24:** 479–85.
13. Revankar C.M., Cimino D.F., Sklar L.A., Arterburn J.B., Prossnitz E.R. (2005) A transmembrane intracellular estrogen receptor mediates rapid cell signaling. *Science* **307:** 1625–30.
14. Thomas P., Pang Y., Filardo E.J., Dong J. (2005) Identity of an estrogen membrane receptor coupled to a G protein in human breast cancer cells. *Endocrinology* **146:** 624–32.
15. Maggiolini M., Picard D. (2010) The unfolding stories of GPR30, a new membrane-bound estrogen receptor. *J Endocrinol* **204:** 105–14.
16. Blight K.J., McKeating J.A., Rice C.M. (2002) Highly permissive cell lines for subgenomic and genomic hepatitis C virus RNA replication. *J Virol* **76:** 13001–14.
17. Lindenbach B.D., Evans M.J., Syder A.J., Wolk B., Tellinghuisen T.L., Liu C.C., Maruyama T., Hynes R.O., Burton D.R., McKeating J.A., Rice C.M. (2005) Complete replication of hepatitis C virus in cell culture. *Science* **309:** 623–6.
18. Bungyoku Y., Shoji I., Makine T., Adachi T., Hayashida K., Nagano-Fujii M., Ide Y.H., Deng L., Hotta H. (2009) Efficient production of infectious hepatitis C virus with adaptive mutations in cultured hepatoma cells. *J Gen Virol* **90:** 1681–91.
19. Deng L., Adachi T., Kitayama K., Bungyoku Y., Kitazawa S., Ishido S., Shoji I., Hotta H. (2008) Hepatitis C virus infection induces apoptosis through a Bax-triggered, mitochondrion-mediated, caspase 3-dependent pathway. *J Virol* **82:** 10,375–85.
20. Stauffer S.R., Coletta C.J., Tedesco R., Nishiguchi G., Carlson K., Sun J., Katzenellenbogen B.S., Katzenellenbogen J.A. (2000) Pyrazole ligands: structure-affinity/activity relationships and estrogen receptor-alpha-selective agonists. *J Med Chem* **43:** 4934–47.
21. Meyers M.J., Sun J., Carlson K.E., Marriner G.A., Katzenellenbogen B.S., Katzenellenbogen J.A. (2001) Estrogen receptor-beta

potency-selective ligands: structure-activity relationship studies of diarylpropionitriles and their acetylene and polar analogues. *J Med Chem* **44:** 4230–51.
22. Bologa C.G., Revankar C.M., Young S.M., Edwards B.S., Arterburn J.B., Kiselyov A.S., Parker M.A., Tkachenko S.E., Savchuck N.P., Sklar L.A., Oprea T.I., Prossnitz E.R. (2006) Virtual and biomolecular screening converge on a selective agonist for GPR30. *Nat Chem Biol* **2:** 207–12.
23. Kasai D., Adachi T., Deng L., Nagano-Fujii M., Sada K., Ikeda M., Kato N., Ide Y.H., Shoji I., Hotta H. (2009) HCV replication suppresses cellular glucose uptake through down-regulation of cell surface expression of glucose transporters. *J Hepatol* **50:** 883–94.
24. Liu Y., Shimizu I., Omoya T., Ito S., Gu X.S., Zuo J. (2002) Protective effect of estradiol on hepatocytic oxidative damage. *World J Gastroenterol* **8:** 363–6.
25. Lu G., Shimizu I., Cui X., Itonaga M., Tamaki K., Fukuno H., Inoue H., Honda H., Ito S. (2004) Antioxidant and antiapoptotic activities of idoxifene and estradiol in hepatic fibrosis in rats. *Life Sci* **74:** 897–907.
26. Inoue H., Shimizu I., Lu G., Itonaga M., Cui X., Okamura Y., Shono M., Honda H., Inoue S., Muramatsu M., Ito S. (2003) Idoxifene and estradiol enhance antiapoptotic activity through estrogen receptor-beta in cultured rat hepatocytes. *Dig Dis Sci* **48:** 570–80.
27. Cooke P.S., Heine P.A., Taylor J.A., Lubahn D.B. (2001) The role of estrogen and estrogen receptor-alpha in male adipose tissue. *Mol Cell Endocrinol* **178:** 147–54.
28. Miyanari Y., Atsuzawa K., Usuda N., Watashi K., Hishiki T., Zayas M., Bartenschlager R., Wakita T., Hijikata M., Shimotohno K. (2007) The lipid droplet is an important organelle for hepatitis C virus production. *Nat Cell Biol* **9:** 1089–97.
29. Watashi K., Inoue D., Hijikata M., Goto K., Aly H.H., Shimotohno K. (2007) Anti-hepatitis C virus activity of tamoxifen reveals the functional association of estrogen receptor with viral RNA polymerase NS5B. *J Biol Chem* **282:** 32,765–72.

ARTICLE
Journal of Cellular Biochemistry 111:676–685 (2010)
Journal of Cellular Biochemistry

E6AP Ubiquitin Ligase Mediates Ubiquitin-Dependent Degradation of Peroxiredoxin 1

Junichi Nasu,[1,2] Kyoko Murakami,[1] Shoji Miyagawa,[3] Ryosuke Yamashita,[3] Tohru Ichimura,[4] Takaji Wakita,[1] Hak Hotta,[3] Tatsuo Miyamura,[1] Tetsuro Suzuki,[1] Tazuko Satoh,[2] and Ikuo Shoji[1,3*]

[1]*Department of Virology II, National Institute of Infectious Diseases, Shinjuku-ku, Tokyo, Japan*

[2]*Department of Oral and Maxillofacial Surgery, School of Life Dentistry at Tokyo, the Nippon Dental University, Chiyoda-ku, Tokyo, Japan*

[3]*Division of Microbiology, Center for Infectious Diseases, Kobe University Graduate School of Medicine, Kobe, Hyogo, Japan*

[4]*Department of Applied Chemistry, National Defense Academy, Yokosuka, Kanagawa, Japan*

ABSTRACT

E6-associated protein (E6AP) is a cellular ubiquitin protein ligase that mediates ubiquitylation and degradation of tumor suppressor p53 in conjunction with the high-risk human papillomavirus E6 protein. We previously reported that E6AP targets annexin A1 protein for ubiquitin-dependent proteasomal degradation. To gain a better understanding of the physiological function of E6AP, we have been seeking to identify novel substrates of E6AP. Here, we identified peroxiredoxin 1 (Prx1) as a novel E6AP-binding protein using a tandem affinity purification procedure coupled with mass spectrometry. Prx1 is a 25-kDa member of the Prx family, a ubiquitous family of antioxidant peroxidases that regulate many cellular processes through intracellular oxidative signal transduction pathways. Immunoprecipitation analysis showed that E6AP binds Prx1 in vivo. Pull-down experiments showed that E6AP binds Prx1 in vitro. Ectopic expression of E6AP enhanced the degradation of Prx1 in vivo. In vivo and in vitro ubiquitylation assays revealed that E6AP promoted polyubiquitylation of Prx1. RNAi-mediated downregulation of endogenous E6AP increased the level of endogenous Prx1 protein. Taken together, our data suggest that E6AP mediates the ubiquitin-dependent proteasomal degradation of Prx1. Our findings raise a possibility that E6AP may play a role in regulating Prx1-dependent intracellular oxidative signal transduction pathways. J. Cell. Biochem. 111: 676–685, 2010.

KEY WORDS: E6AP; Prx1; UBIQUITIN; DEGRADATION

E6-associated protein (E6AP) is the prototype of a family of ubiquitin ligases called HECT domain ubiquitin ligases, all of which contain a domain homologous to the E6AP carboxyl terminus [Huibregtse et al., 1995]. E6AP was initially identified as the cellular factor that stimulates ubiquitin-dependent degradation of the tumor suppressor p53 in conjunction with the E6 protein of cervical cancer-associated human papillomavirus (HPV) types 16 and 18 [Huibregtse et al., 1993; Scheffner et al., 1994]. The E6–E6AP complex functions as an E3 ubiquitin ligase in the ubiquitylation of p53 [Scheffner et al., 1993]. Known substrates of the E6–E6AP complex include the tumor suppressor p53 [Scheffner et al., 1993], the PDZ domain-containing protein Scribble [Nakagawa and Huibregtse, 2000], and NFX1-91, a transcriptional repressor of the gene encoding hTERT [Gewin et al., 2004]. The ability of E6 to

Abbreviations: E6AP, E6-associated protein; Prx, peroxiredoxin; HPV, human papillomavirus; MS, mass spectrometry; MAb, monoclonal antibody; PAb, polyclonal antibody; GAPDH, glyceraldehydes-3-phosphate dehydrogenase; CHX, cycloheximide.

Grant sponsor: The Nippon Dental University; Grant sponsor: Japan Health Sciences Foundation; Grant sponsor: Ministry of Health, Labour, and Welfare; Grant sponsor: Ministry of Education, Science and Culture of Japan; Grant sponsor: Program for Promotion of Fundamental Studies in Health Sciences of the National Institute of Biomedical Innovation (NIBIO), Japan.

*Correspondence to: Dr. Ikuo Shoji, MD, PhD, Division of Microbiology, Center for Infectious Diseases, Kobe University Graduate School of Medicine, 7-5-1 Kusunoki-cho, Chuo-ku, Kobe, Hyogo 650-0017, Japan.
E-mail: ishoji@med.kobe-u.ac.jp

Received 7 March 2010; Accepted 15 June 2010 • DOI 10.1002/jcb.22752 • © 2010 Wiley-Liss, Inc.
Published online 29 June 2010 in Wiley Online Library (wileyonlinelibrary.com).

utilize E6AP to target p53 and other cellular proteins for degradation contributes to its oncogenic functions [Matentzoglu and Scheffner, 2008]. Interestingly, E6AP is not involved in the ubiquitylation of p53 in the absence of E6 [Talis et al., 1998].

In an attempt to understand the physiological function of E6AP, several potential E6-independent substrates for E6AP have been identified, such as HHR23A and HHR23B (the human orthologs of *Saccharomyces cerevisae* Rad23) [Kumar et al., 1999], Blk (a member of the Src family kinases) [Oda et al., 1999], Mcm7 (which is involved in DNA replication) [Kuhne and Banks, 1998], trihydrophobin 1 [Yang et al., 2007], and AIB1 (a steroid receptor coactivator) [Mani et al., 2006]. We previously reported that E6AP mediates ubiquitylation and degradation of annexin A1 in a Ca^{2+}-dependent manner [Shimoji et al., 2009].

Some patients with Angelman syndrome, a severe neurological disorder linked to E6AP, have mutations within the catalytic cleft that have been shown to reduce E6AP ubiquitin ligase activity [Kishino et al., 1997; Matsuura et al., 1997; Cooper et al., 2004]. Despite the significant progress in the study of Angelman syndrome-associated E6AP mutations, none of the identified E6AP substrates have been directly linked to the disorder. Much research is still needed to fully understand the functional links between lack of E6AP expression and clinical manifestations of Angelman syndrome [Dan, 2009]. We previously reported that E6AP mediates ubiquitin-dependent proteasomal degradation of hepatitis C virus (HCV) core protein, thereby affecting the production of HCV particles [Shirakura et al., 2007; Suzuki et al., 2009]. It is becoming increasingly clear that E6AP plays important roles in human diseases, such as cervical cancer, Angelman syndrome, and hepatitis C [Scheffner et al., 1993; Kishino et al., 1997; Shirakura et al., 2007].

In this study, we attempted to identify the novel functions of E6AP. We screened for potential binding partners for E6AP. A tandem affinity purification procedure coupled with mass spectrometry analysis identified peroxiredoxin 1 (Prx1) as a novel binding partner for E6AP. We provide evidence suggesting that E6AP mediates the ubiquitin-dependent proteasomal degradation of Prx1.

MATERIALS AND METHODS

CELL CULTURE AND TRANSFECTION

Human embryonic kidney (HEK) 293T cells were cultured in Dulbecco's modified Eagle's medium (DMEM; Sigma-Aldrich, St. Louis, MO) supplemented with 50 IU/ml penicillin, 50 μg/ml streptomycin (Invitrogen, Carlsbad, CA), and 10% (v/v) fetal bovine serum (FBS; JRH Biosciences, Lenexa, KS) at 37°C in a 5% CO_2 incubator. HEK293T cells were transfected with plasmid DNA using TransIT-LT1 (Mirus, Madison, WI).

PLASMIDS AND RECOMBINANT BACULOVIRUSES

To make a fusion protein consisting of hexahistidine (His_6)-tag fused to the N-terminus of Prx1 in *Escherichia coli*, pET17b-Prx1 [Kang et al., 1998] was digested with *Nde*I and *Bam*HI, and a Prx1 fragment was subcloned into the *Nde*I-Bpu1120I site of pET19b, resulting in pET19b-Prx1. The expression plasmid pET19b-Prx2 was constructed similarly. The plasmids, pET17b-Prx1 and pET17b-Prx2, were kind gifts from Dr. S.G. Rhee, Ewha Women's University, Korea.

To express the Prx1 protein as a FLAG-tagged fusion protein in mammalian cells, pCAG-FLAG-Prx1 was constructed as follows. The DNA fragment of Prx1 was amplified from pET17b-PrxI by polymerase chain reaction (PCR) using two oligonucleotides, 5′-GCGGCCGCCCACCATGGACTACAAAGACGATGACGATAAAGG-AGGCGGCGGATCCATGTCTTCAGGAAATGC-3′ and 5′-AGATCTT-CACTTCTGCTTGGAG-3′. To express FLAG-tagged Prx2 protein in mammalian cells, the DNA fragment of Prx2 was amplified from pET17b-Prx2 by PCR using two oligonucleotides, 5′-GCGGCCG-CCCACCATGGACTACAAAGACGATGACGATAAAGGAGGCGGCG-GATCCATGGCCTCCGGTAACGC-3′ and 5′-AGATCTCTAATTGTG-TTTGGAG-3′. The amplified PCR fragments were subcloned into pGEM T-Easy (Promega, Madison, WI) and verified by sequencing. Then the Prx1 and Prx2 gene fragments were digested with *Not*I and *Bgl*II, and ligated into the *Not*I–*Bgl*II site of pCAG-MCS2 [Shirakura et al., 2007]. The MEF-tag cassette (containing Myc-tag, the tobacco etch virus protease cleavage site, and FLAG-tag) was fused to the N-terminus of the cDNA encoding E6AP [Ichimura et al., 2005; Shirakura et al., 2007]. MEF-tagged E6AP and MEF-tagged E6AP C-A were subcloned into pcDNA3, pCAGGS, and pVL1392. pCAG-HA-E6AP, pCAG-HA-E6AP C-A, and pCAG-HA-Nedd4 were described previously [Shirakura et al., 2007; Shimoji et al., 2009]. The ubiquitin expression plasmids, pRK5-HA-Ubiquitin wild type (WT), pRK5-HA-Ubiquitin-K48R, and pRK5-HA-Ubiquitin-K48 [Lim et al., 2005], were provided by Dr. T. Dawson (Johns Hopkins University, MD).

ANTIBODIES

The mouse monoclonal antibodies (MAbs) used in this study were anti-hemagglutinin (HA) MAb (12CA5; Roche, Mannheim, Germany), anti-HA MAb (16B12; Covance, Princeton, NJ), anti-FLAG M2 mouse MAb (Sigma-Aldrich), anti-glyceraldehyde-3-phosphate dehydrogenase (GAPDH) MAb (Chemicon, Temecula, CA), anti-E6AP MAb (E6AP-330; Sigma-Aldrich), and anti-polyhistidine (His-1) MAb (Sigma-Aldrich). The c-Myc tagged protein mild purification kit (MBL) was used for immunoprecipitation. The polyclonal antibodies (PAbs) used in this study were anti-HA rabbit PAb (Y-11; Santa Cruz Biotechnology, Santa Cruz, CA), anti-FLAG rabbit PAb (F7425; Sigma-Aldrich), anti-Prx1 rabbit PAb (ab16805-100) (Abcam, Cambridge, Oxford), and anti-GST goat PAb (Amersham, Buckinghamshire, UK).

EXPRESSION AND PURIFICATION OF RECOMBINANT PROTEINS

E. coli BL21 (DE3) cells were transformed with plasmids expressing His_6-tagged protein and grown at 37°C. Expression of the fusion protein was induced by 1 mM isopropyl-β-D-thiogalactopyranoside (IPTG) at 25°C for 4 h. Bacteria were harvested, suspended in lysis buffer [50 mM Na_2HPO_4, 300 mM NaCl, 5 mM Imidazole, 0.1% Triton X-100, protease inhibitor cocktail (Complete EDTA-free; Roche)], and sonicated on ice. His_6-tagged proteins were purified on Ni-NTA beads (Qiagen, Hilden, Germany) according to the manufacturer's protocols. The MEF-E6AP and MEF-E6AP C-A were purified on anti-FLAG M2 agarose beads (Sigma-Aldrich) as described previously [Shirakura et al., 2007].

PURIFICATION OF E6AP-BINDING PROTEINS BY MEF PURIFICATION PROCEDURE

HEK293T cells were transfected with the plasmid expressing MEF-E6AP C-A by the calcium phosphate precipitation method, and the E6AP-binding proteins were recovered following the procedure described previously [Ichimura et al., 2005]. The inactive form of E6AP was expressed to inhibit ubiquitin-dependent degradation of potential substrates. Bound proteins were separated by 7.5% sodium dodecyl sulfate-polyacrylamide gel electrophoresis (SDS-PAGE) and visualized by silver staining. The stained bands were excised and digested in the gel with lysylendoprotease-C (Lys-C), and the resulting peptide mixtures were analyzed using a direct nanoflow liquid chromatography-tandem mass spectrometry (MS/MS) system, equipped with an electrospray interface reversed-phase column, a nanoflow gradient device, a high-resolution Q-time of flight hybrid mass spectrometer (Q-TOF2; Micromass, Manchester, UK), and an automated data analysis system [Natsume et al., 2002; Shirakura et al., 2007]. All the MS/MS spectra were searched against the nonredundant protein sequence database maintained at the National Center for Biotechnology Information using the Mascot program (Matrix Science, London, UK) to identify proteins. The MS/MS signal assignments were also confirmed manually.

Ni-NTA PULL-DOWN ASSAY

For Ni-NTA pull-down assays, purified MEF-E6AP was incubated with His_6-Prx proteins immobilized on Ni-NTA agarose beads (Qiagen) in 1 ml of the binding buffer [50 mM Tris-HCl (pH 7.5), 10% glycerol, 1% Triton X-100, 150 mM NaCl, 5 μM $ZnCl_2$, 1 mM Na_3VO_4, 10 mM EGTA, protease inhibitor cocktail (Complete EDTA-free)] at 4°C for 30 min. The beads were washed four times with wash buffer [50 mM Na_2HPO_4, 300 mM NaCl, 50 mM Imidazole, 0.1% Triton X-100, protease inhibitor cocktail (Complete EDTA-free)], and the pull-down complexes were separated by SDS-PAGE on 12.5% polyacrylamide gels and analyzed by immunoblotting with anti-FLAG MAb and anti-polyhistidine (His-1) MAb.

IMMUNOFLUORESCENCE MICROSCOPY

Cells were transfected with pCAG-HA-E6AP C-A and pCAG-FLAG-Prx1 using TransIT-LT1 according to the manufacturer's instructions. Transfected cells grown on collagen-coated coverslips were washed with PBS, fixed with 4% paraformaldehyde for 30 min at 4°C, and permeabilized with PBS containing 2% FCS and 0.3% Triton X-100. Cells were incubated with anti-HA mouse MAb and anti-FLAG rabbit PAb as primary antibodies, washed, and incubated with Alexa Fluor 488 goat anti-mouse IgG (Molecular Probes, Eugene, OR) and Alexa Fluor 555 goat anti-rabbit IgG (Molecular Probes) as secondary antibodies. Then, the cells were washed with PBS, mounted on glass slides, and examined with a BZ-8000 microscope (Keyence).

siRNA TRANSFECTION

HEK293T cells (3×10^5 cells in a six-well plate) were transfected with 40 pmol of either E6AP-specific small interfering RNA (siRNA; Sigma-Aldrich), or scramble negative-control siRNA duplexes (Sigma-Aldrich) using HiPerFect transfection reagent (Qiagen) following the manufacturer's instructions. The E6AP-siRNA target sequences were as follows:

siE6AP-1 (sense), 5′-GGGUCUACACCAGAUUGCUTT-3′; scramble negative control (siCont-1, sense), 5′-UUGCGGGUCUAAUCACCGATT-3′ [Shirakura et al., 2007].

IN VIVO UBIQUITYLATION ASSAY

In vivo ubiquitylation assays were performed essentially as described previously [Shirakura et al., 2007]. Where indicated, cells were treated with 25 μM MG132 (Calbiochem, La Jolla, CA) or with dimethylsulfoxide (DMSO; control) for 30 min prior to collection. FLAG-Prx1 was immunoprecipitated with anti-FLAG MAb. Immunoprecipitates were analyzed by immunoblotting, using either anti-HA PAb or anti-FLAG MAb to detect ubiquitylated Prx1.

IN VITRO UBIQUITYLATION ASSAY

In vitro ubiquitylation assays were performed essentially as described previously [Shirakura et al., 2007]. For in vitro ubiquitylation of Prx1, purified His_6-Prx1 was used as a substrate. Assays were done in 40-μl volumes containing 20 mM Tris-HCl, pH 7.6, 50 mM NaCl, 5 mM $MgCl_2$, 5 mM ATP, 8 μg of bovine ubiquitin (Sigma-Aldrich), 0.1 mM DTT, 200 ng of mouse E1, 200 ng of E2 (UbcH7), and 0.5 μg of MEF-E6AP. The reaction mixtures were incubated at 37°C for 120 min followed by immunoprecipitation with anti-Prx1 PAb. The samples were analyzed by immunoblotting with anti-Ub MAb.

RESULTS

IDENTIFICATION OF Prx1 AS A BINDING PARTNER FOR E6AP

To identify novel substrates for E6AP, we screened for E6AP-binding proteins using a tandem affinity purification procedure with a tandem tag (known as MEF-tag) [Ichimura et al., 2005; Shirakura et al., 2007]. Seven proteins were reproducibly detected from lysed cells transfected with MEF-E6AP C-A (Fig. 1A, lane 2), but none were recovered from lysed control cells transfected with empty vector alone (Fig. 1A, lane 1). To identify the proteins, silver-stained bands were excised from the gel, digested with Lys-C, and analyzed using a direct nanoflow liquid chromatography-MS/MS system. One of these bands, migrating at 25 kDa (Fig. 1A, lane 2, No. 7), was identified as Prx1 based on two independent MS spectra (Fig. 1B,C). To confirm the proteomic identification of Prx1, HEK293T cells were transfected with MEF-E6AP C-A plasmid or empty plasmid. The cells were lysed and immunoprecipitated with anti-Myc MAb or control IgG. Endogenous Prx1 was co-immunoprecipitated with anti-Myc MAb, suggesting that E6AP binds endogenous Prx1 (Fig. 1D, lane 4).

IN VIVO INTERACTION BETWEEN Prx1 AND E6AP

To determine whether E6AP specifically interacts with Prx1, HA-E6AP plasmid was introduced into HEK293T cells together with either FLAG-Prx1 plasmid or FLAG-Prx2 plasmid. Prx1 and Prx2 share 77.4% sequence identity at the protein level. Cells were lysed and immunoprecipitated with anti-HA MAb, anti-FLAG MAb, or

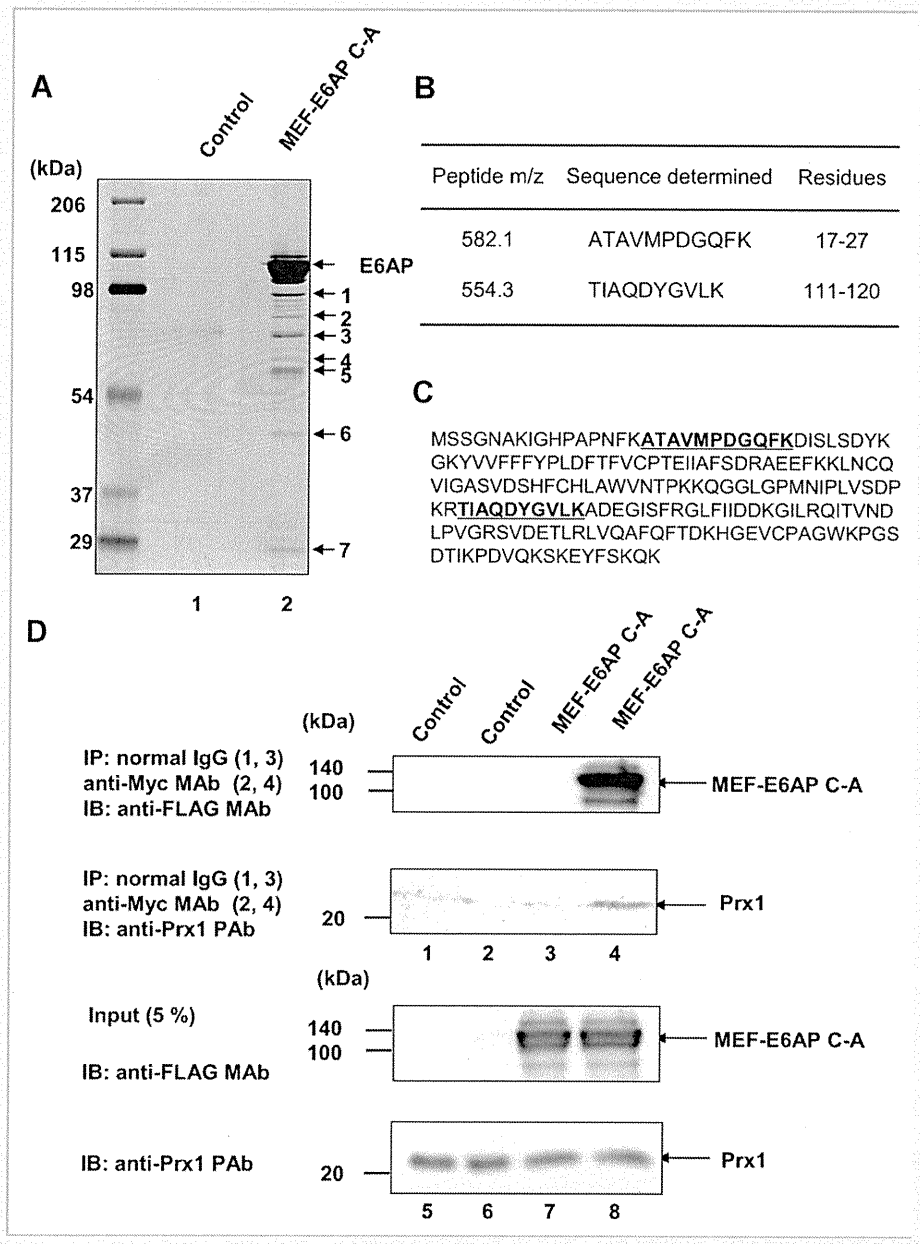

Fig. 1. Identification of Prx1 as a binding partner for E6AP. A: Prx1 interacts with E6AP in vivo. HEK293T cells were transfected with pcDNA3-MEF-E6AP C-A or empty plasmid, incubated for 48 h, and then harvested. The expressed MEF-E6AP C-A and binding proteins were recovered using the MEF purification procedure. Proteins bound to the MEF-E6AP C-A immobilized on anti-FLAG beads were dissociated with FLAG peptides, resolved by 7.5% SDS–PAGE, and visualized by silver staining. Control experiments were performed using HEK293T cells transfected with vector alone. Bound proteins were detected by SDS–PAGE and silver staining. Molecular weight markers are indicated as well as the position of p25 (No. 7), which likely corresponds to Prx1. B: Peptide masses were identified by tandem mass spectrometry. The protein was Prx1 (GenBank accession No. BC021683). C: Corresponding amino acids of Prx1 (peptides in bold print). D: HEK293T cells were co-transfected with MEF-E6AP C-A plasmid. Control experiments were performed using HEK293T cells transfected with vector alone. Cell lysates were immunoprecipitated with anti-Myc MAb or normal mouse IgG (lanes 1–4), eluted with c-Myc tag peptide. Eluates were analyzed by immunoblotting with anti-FLAG MAb or anti-Prx1 PAb. The input samples were separated by SDS–PAGE and analyzed by immunoblotting with anti-FLAG MAb or anti-Prx1 PAb (lanes 5–8). The positions of Prx1 and MEF-E6AP C-A are indicated by arrows. IB, immunoblot; IP, immunoprecipitation.

normal IgG (Fig. 2A, lanes 1–6). FLAG-Prx1 but not FLAG-Prx2 was co-immunoprecipitated with anti-HA MAb (Fig. 2A, lower panel, lanes 1 and 2). Conversely, HA-E6AP was co-immunoprecipitated with FLAG-Prx1 but not FLAG-Prx2 using anti-FLAG MAb (Fig. 2A, upper panel, lanes 3 and 4). These results suggest that E6AP specifically interacts with Prx1.

To determine whether Prx1 and E6AP co-localize in the cells, immunofluorescence microscopy analysis was performed in HEK293T cells. There was no staining without primary antibodies (data not shown). The immunofluorescence study showed that E6AP and Prx1 mainly localize in the cytoplasm and that E6AP and Prx1 co-localize in the cytoplasm (Fig. 2B, Merge).

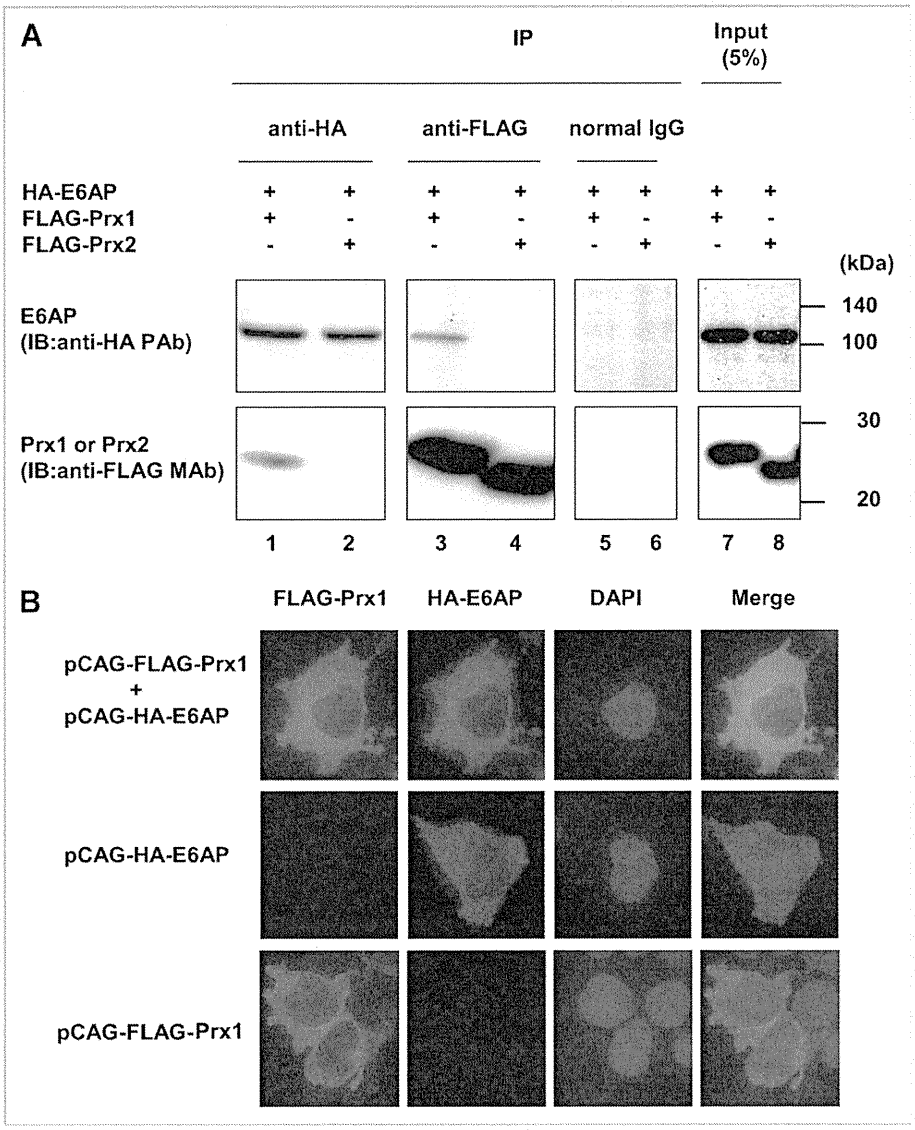

Fig. 2. In vivo interaction between Prx1 and E6AP. A: HEK293T cells were co-transfected with pCAG-HA-E6AP together with either pCAG-FLAG-Prx1 or pCAG-FLAG-Prx2. Cell lysates were immunoprecipitated with anti-HA mouse MAb, anti-FLAG mouse MAb, or normal mouse IgG and analyzed by immunoblotting with anti-HA PAb or anti-FLAG MAb. B: HEK293T cells were transfected with either HA-E6AP plasmid or FLAG-Prx1 plasmid, grown on coverslips, fixed, and processed for double-label immunofluorescence for HA-E6AP or FLAG-Prx1. All the samples were examined with a BZ-8000 microscope (Keyence).

IN VITRO INTERACTION BETWEEN Prx1 AND E6AP

To determine whether E6AP interacts with Prx1 in vitro, purified recombinant MEF-E6AP, MEF-annexin A1 expressed in insect cells using a baculovirus system and purified recombinant His_6-Prx1 and His_6-Prx2 expressed in *E. coli* were used. The His_6-tagged Prx proteins were mixed with either MEF-E6AP or MEF-annexin A1, incubated, pulled down with Ni-NTA agarose, and analyzed by immunoblotting with anti-FLAG MAb (Fig. 3, upper panel) or anti-polyhistidine MAb (Fig. 3, middle panel). MEF-annexin A1 served as a negative control to confirm that MEF-tag does not bind Prx1. MEF-E6AP was pulled down with Prx1, but not with Prx2 (Fig. 3, lanes 1 and 3), whereas annexin A1 was not pulled down with either Prx1 or Prx2 (Fig. 3, lanes 2 and 4). These results suggest that E6AP directly and specifically binds Prx1 in vitro.

E6AP DECREASES STEADY-STATE LEVELS OF Prx1 IN HEK293T CELLS

One of the characteristic features of HECT domain ubiquitin ligases is their direct association with their substrates. Thus, we hypothesized that E6AP would function as an E3 ubiquitin ligase for Prx1. We assessed the effects of E6AP on the steady-state levels of Prx1 in HEK293T cells. FLAG-Prx1 together with HA-tagged E6AP, catalytically inactive E6AP, E6AP C-A, or Nedd4 (another HECT domain ubiquitin ligase) was introduced into HEK293T cells, and the levels of Prx1 were examined by immunoblotting. The steady-state

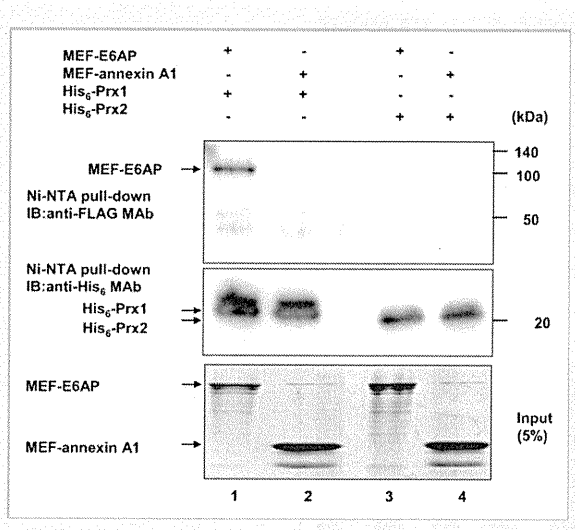

Fig. 3. In vitro interaction between Prx1 and E6AP. Purified MEF-E6AP, MEF-Annexin A1, His_6-Prx1, and His_6-Prx2 were used to examine the interaction between E6AP and Prxs. Purified MEF-E6AP was mixed with either His_6-Prx1 or His_6-Prx2, incubated, and pulled down with Ni-NTA agarose. MEF-Annexin A1 served as a negative control. The bound proteins were separated by SDS-PAGE and analyzed by immunoblotting with anti-FLAG MAb (upper panel) or anti-His_6 MAb (middle panel). The input MEF-E6AP and MEF-annexin A1 were separated by SDS-PAGE and stained with Coomassie brilliant blue (lower panel).

levels of Prx1 decreased with an increase in the amount of E6AP plasmid (Fig. 4A lanes 1–3, Fig. 4B). However, neither E6AP C-A nor Nedd4 decreased the steady-state levels of Prx1 (Fig. 4A lanes 4–6 and 7–9, Fig. 4B), indicating that E6AP specifically decreases Prx1.

To determine if endogenous E6AP is critical for the degradation of endogenous Prx1 in the cells, the expression of E6AP was knocked down by siRNA and the expression of Prx1 and E6AP was analyzed by immunoblotting. Transfection of siE6AP into HEK293T cells resulted in a decrease in E6AP levels by 97% (Fig. 4C, upper panel, lane 2). Knock-down of endogenous E6AP resulted in accumulation of endogenous Prx1 (Fig. 4C, lane 2, middle panel), suggesting that endogenous E6AP plays a role in the proteolysis of endogenous Prx1.

To further investigate if the E6AP-induced reduction of Prx1 is dependent on the proteasome, we examined the effects of the proteasome inhibitor clasto-lactacystin and the lysosomal enzyme inhibitors, E-64d and Pepstatin A, on the level of Prx1. Clasto-lactacystin was used to examine if Prx1 gets stabilized after the treatment, because it has an irreversible inhibitory effect on proteasome. HEK293T cells were transfected with pCAG-FLAG-Prx1 plus either empty vector or pCAG-HA-E6AP. Overexpression of E6AP resulted in a remarkable reduction of the Prx1 (Fig. 4D, lane 2, middle panel), whereas the Prx1 protein level was increased after treatment with clasto-lactacystin (Fig. 4D, lane 4, middle panel). In contrast, the Prx1 protein level was unchanged after treatment with E-64d plus Pepstatin A (Fig. 4D, lane 6, middle panel). These results indicate that E6AP-induced reduction of Prx1 is proteasome-dependent.

E6AP-DEPENDENT POLYUBIQUITYLATION OF Prx1 IN VIVO

To determine whether E6AP can induce ubiquitylation of Prx1 in cells, we performed in vivo ubiquitylation assays. HEK293T cells were transfected with FLAG-Prx1 plasmid and either E6AP or Nedd4 plasmid, together with a plasmid encoding HA-tagged ubiquitin to facilitate the detection of ubiquitylated Prx1. Cell lysates were immunoprecipitated with anti-FLAG MAb and immunoblotted with anti-HA PAb to detect ubiquitylated Prx1 protein. No ubiquitin signal was detected in the cells co-transfected with empty plasmid or Nedd4 plasmid (Fig. 5A, lanes 4 and 6). In contrast, co-expression of E6AP led to readily detectable polyubiquitylated forms of the Prx1 as a smear of higher-molecular weight bands (Fig. 5A, left panel, lane 5). Immunoblot analysis with anti-FLAG PAb confirmed that FLAG-Prx1 was immunoprecipitated and that higher-molecular weight bands conjugated with HA-ubiquitin were indeed poly-ubiquitylated forms of the FLAG-Prx1 (Fig. 5A, right panel, lane 5). These results suggest that E6AP enhances polyubiquitylation of Prx1 in vivo.

To further investigate if E6AP is involved in K48-linked ubiquitylation of Prx1, we performed in vivo ubiquitylation assay using HA-tagged K48R dominant negative ubiquitin mutant and K48 only ubiquitin mutant expression plasmids. HEK293T cells were transfected with FLAG-Prx1 plasmid and E6AP plasmid, together with a plasmid encoding HA-ubiquitin WT, HA-K48R ubiquitin, or HA-K48 ubiquitin to facilitate the detection of ubiquitylated Prx1. Ubiquitin signal was detected in the cells transfected with either HA-ubiquitin WT or HA-K48 ubiquitin plasmid (Fig. 5B, lane 1 or 3), whereas no ubiquitin signal was detected in the cells transfected with HA-K48R ubiquitin (Fig. 5B, lane 2), suggesting that E6AP enhances K48-linked polyubiquitylation of Prx1. These results are consistent with the notion that E6AP is involved in proteasomal degradation of Prx1.

E6AP MEDIATES POLYUBIQUITYLATION OF Prx1 IN VITRO

To reconstitute the E6AP-mediated polyubiquitylation of Prx1 in vitro, we performed an in vitro ubiquitylation assay of the Prx1 using purified MEF-E6AP and His_6-Prx1 as described above. When the in vitro ubiquitylation reaction was carried out in the presence of MEF-E6AP C-A, no ubiquitylation signal was detected (Fig. 5C, lanes 3). However, inclusion of purified MEF-E6AP in the reaction mixture resulted in ubiquitylation of His_6-Prx1 (Fig. 5C, lane 4). No signal was detected when His_6-Prx1 was not included in the reaction mixture (Fig. 5C, lane 2). From these results, we concluded that E6AP mediates polyubiquitylation of Prx1.

DISCUSSION

In this study, we identified Prx1 as a novel E6AP-binding protein using a tandem affinity purification procedure coupled with mass spectrometry. Overexpression of E6AP enhances proteasomal degradation of Prx1, and siRNA-mediated knockdown of endogenous E6AP results in accumulation of endogenous Prx1. E6AP enhances the polyubiquitylation of Prx1 in vivo and in vitro. We conclude that E6AP mediates ubiquitin-dependent degradation of

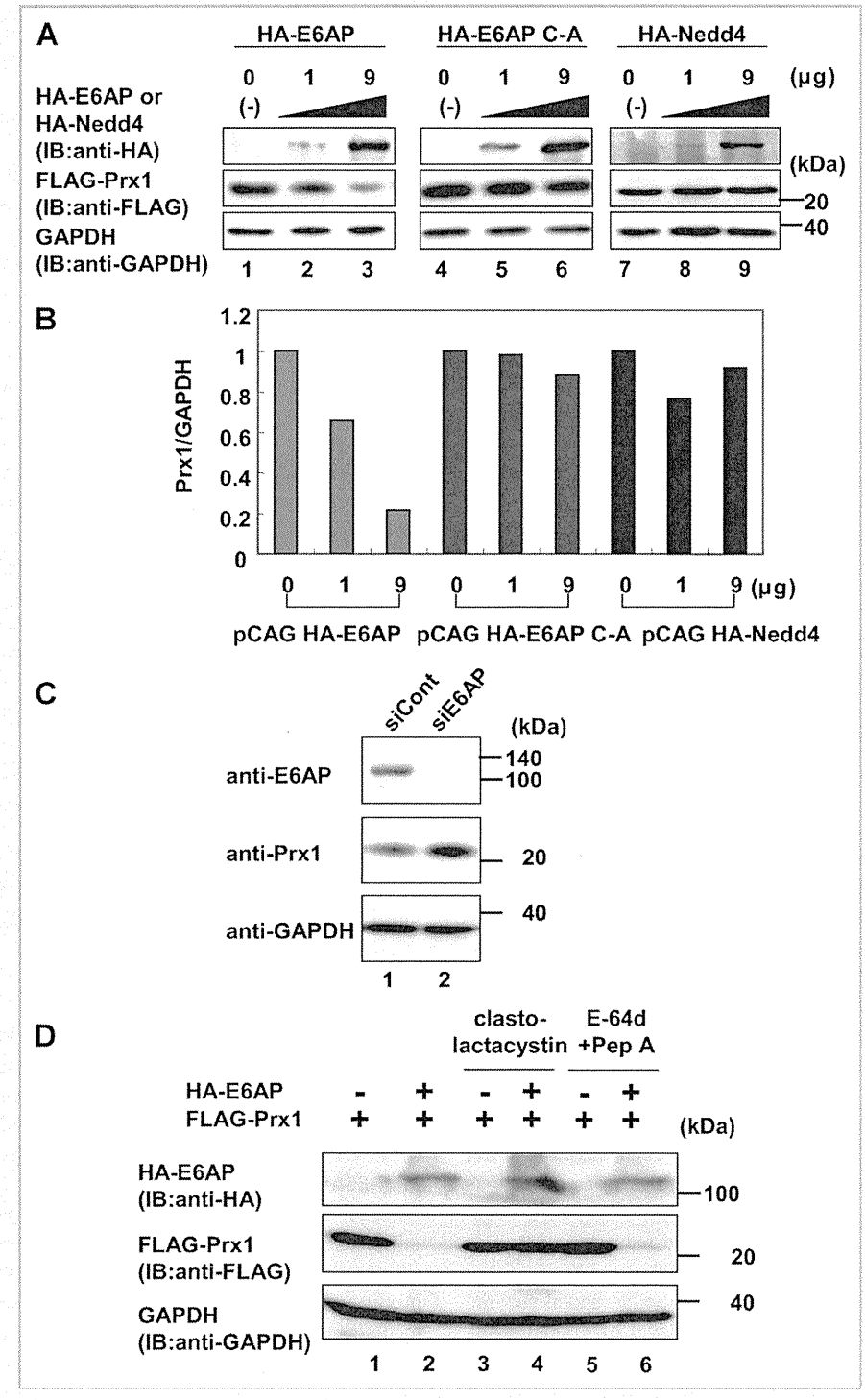

Fig. 4. E6AP decreases the steady-state levels of Prx1 protein in HEK293T cells. A: HEK293T cells (5×10^5 cells/six-well plate) were transfected with 0.5 μg pCAG-FLAG-Prx1 plus empty vector and 1 or 9 μg of pCAG-HA-E6AP, pCAG-HA-E6AP C-A, or pCAG-HA-Nedd4. At 48 h posttransfection, equivalent amounts of the whole-cell lysates were separated by SDS-PAGE and analyzed by immunoblotting with anti-HA MAb (top panel), anti-FLAG MAb (middle panel), and anti-GAPDH MAb (bottom panel). The results shown are representative of three independent experiments. B: Quantitation of the data shown in panel A. The intensities of the gel bands were quantitated using the ImageJ 1.43 program. The level of GAPDH served as a loading control. C: Knockdown of endogenous E6AP by siRNA resulted in the accumulation of endogenous Prx1 in HEK293T cells. HEK293T cells (3×10^5 cells/six-well plate) were transfected with 40 pmol of E6AP-specific duplex siRNA (or a scramble negative control). The cells were harvested at 96 h after siRNA transfection. D: HEK293T cells (5×10^5 cells/six-well plate) were transfected with 0.5 μg of pCAG-FLAG-Prx1 plus 9 μg of empty vector or pCAG-HA-E6AP. At 36 h after transfection, the cells were treated with DMSO control (lanes 1 and 2), 30 μM clasto-lactacystin (lanes 3 and 4), or 40 μM E-64d plus 20 μM Pepstatin A (lanes 5 and 6). Cells were collected at 12 h after treatment with the inhibitors. Equivalent amounts of the whole-cell lysates were separated by SDS-PAGE and analyzed by immunoblotting with anti-HA MAb (upper panel), anti-FLAG MAb (middle panel), or anti-GAPDH MAb (lower panel).

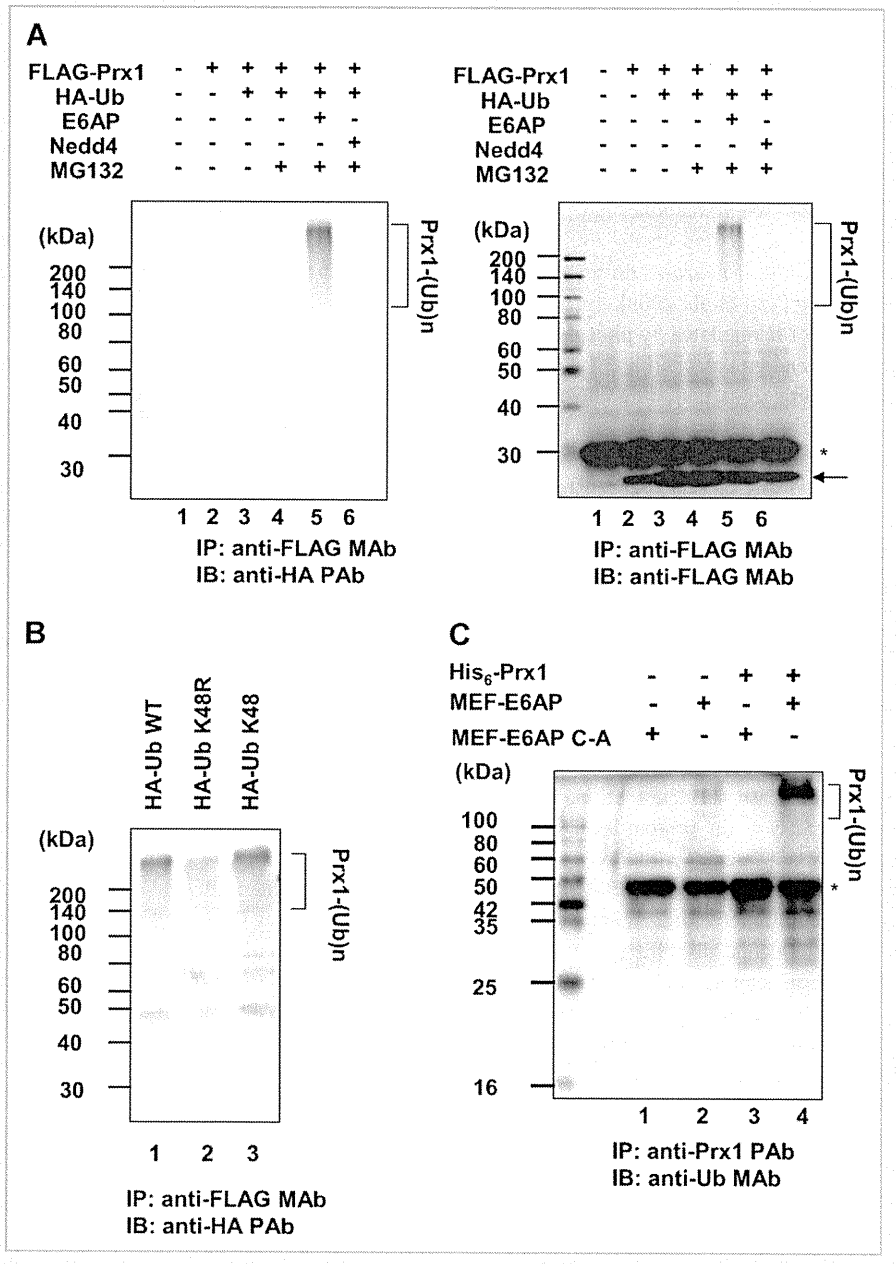

Fig. 5. E6AP mediates ubiquitylation of Prx1 in vivo and in vitro. A: HEK293T cells (2×10^6 cells/10-cm dish) were transfected with 1 μg of pCAG-FLAG-Prx1 together with 2 μg of plasmid encoding E6AP or Nedd4 as indicated. Each transfection also included 2 μg of plasmid encoding HA-ubiquitin. The cell lysates were immunoprecipitated with FLAG beads and analyzed by immunoblotting with anti-HA PAb (left panel) or anti-FLAG MAb (right panel). Arrow indicates FLAG-Prx1. Asterisk indicates immunoglobulin light chain. Ubiquitylated species of FLAG-Prx1 are marked by brackets. B: HEK293T cells (2×10^6 cells/10-cm dish) were transfected with 1 μg of pCAG-FLAG-Prx1 together with 2 μg of plasmid encoding E6AP plasmid. Each transfection also included 2 μg of plasmid encoding HA-Ub WT, HA-Ub K48R, or HA-Ub K48 as indicated. At 36 h after transfection, the cells were treated with 25 μM MG132 and cultured for 12 h. The cell lysates were immunoprecipitated with FLAG beads and analyzed by immunoblotting with anti-HA PAb. Ubiquitylated species of FLAG-Prx1 are marked by brackets. C: In vitro ubiquitylation of Prx1 by recombinant E6AP. For in vitro ubiquitylation of Prx1 protein, purified His_6-Prx1 was used as a substrate. Assays were done in 40-μl volumes containing each component as indicated. The reaction mixture is described in Materials and Methods Section. The reaction was carried out at 37°C for 120 min followed by immunoprecipitation with anti-Prx1 PAb and analysis by immunoblotting with anti-Ub MAb. Ubiquitylated species of His_6-Prx1 are marked by brackets. Asterisk indicates immunoglobulin heavy chain.

Prx1. Our results suggest that E6AP is involved in the regulation of Prx1 activity through the ubiquitin-proteasome pathway.

Prx1 is a 25-kDa member of the Prx family, a ubiquitous family of antioxidant peroxidases that regulate many cellular processes through intracellular oxidative signal transduction pathways. More than 50 members of the Prx family have been identified in a wide variety of organisms ranging from prokaryotes to mammals. Prxs are widely expressed hydrogen peroxide scavenger proteins best

known for their role in detoxifying reactive oxygen species, DNA damage, and cancer, but they also act in cellular signaling and as molecular chaperones [Jang et al., 2004; Hall et al., 2009]. Mammalian cells express six isoforms of Prx (Prx1–6), which are classified into three subgroups (2-Cys, atypical 2-Cys, and 1-Cys) [Rhee et al., 2005]. Prx1 is a 2-Cys thiol reductase that forms a component of cellular antioxidant and thermal stress defense mechanisms through its ability to metabolize H_2O_2, and its properties as a molecular chaperone [Wood et al., 2003a,b; Jang et al., 2004]. Furthermore, Prx1 controls neuronal differentiation by a thiol-redox-dependent cascade [Yan et al., 2009].

The peroxidase activity of Prx1 is regulated by phosphorylation, which is mediated by cyclin-dependent kinases [Chang et al., 2002]. Phosphorylation at Thr90 by several Cdks, including Cdc2, results in inhibition of its peroxidase activity. Another known regulatory mechanism is cysteine sulfinic acid formation [Woo et al., 2003]. The active-site cysteine of Prx1 is selectively reduced to cysteine sulfinic acid during catalysis, which leads to inactivation of peroxidase activity. Reversing the inactivation of Prx1 was previously identified as a mechanism for its regulation. The sulfinic form of Prx1, produced during the exposure of cells to H_2O_2, is rapidly reduced to the catalytic active thiol form [Woo et al., 2003]. We propose here a novel regulatory mechanism of Prx1. Our results show for the first time that the E6AP-mediated ubiquitin–proteasome pathway is a mechanism for irreversibly attenuating the activity of Prx1. Our data suggest that E6AP specifically targets Prx1 for ubiquitin-dependent proteasomal degradation. Prx1 and Prx2 share 77.4% sequence identity at the protein level. However, our data showed that E6AP does not interact with Prx2 in vivo and in vitro, suggesting a specific interaction between E6AP and Prx1.

Angelman syndrome is a neurologic disorder characterized by developmental delay, severe intellectual disability, motor impairment, absent speech, happy demeanor, and epilepsy, and is attributed to an absence of UBE3A/E6AP gene expression that may be caused by various abnormalities of chromosome 15. Although the genetic link between UBE3A/E6AP and Angelman syndrome was identified more than 13 years ago [Kishino et al., 1997; Matsuura et al., 1997], the underlying pathophysiology is poorly understood. Ubiquitin-mediated proteolysis may be important in a number of processes of neuronal development, including synaptogenesis and mechanisms of long-term memory. Recent findings in animal models of Angelman syndrome have demonstrated altered dendritic spine formation as well as both synaptic and nonsynaptic influences in various brain regions, including hippocampus and cerebellar cortex [Dan, 2009]. Yan et al. [2009] provided several lines of evidence suggesting that the requirement for Prx1 in motor neuron differentiation stems from a previously uncharacterized enzymatic function that is distinct from its molecular chaperone or H_2O_2 metabolic activities. It may be intriguing to investigate the functional link between lack of UBE3A/E6AP expression and stability of Prx1 with regard to the pathogenesis of Angelman syndrome.

The expression of Prx1 is induced by oxidative stress including that from the exposure to O^2, Fe^{3+}, or 2-mercaptoethanol. In addition to H_2O_2, other chemicals such as phorbol ester and okadaic acid have also been shown to induce the expression of Prx1 [Immenschuh et al., 2002; Wijayanti et al., 2008]. Increased expression of Prx1, in turn, contributes to greater resistance to oxidative stress. Many studies have indicated that aberrant expression of Prx1 was found in various kinds of cancers, such as thyroid tumors, oral cancers, lung cancers, and esophageal carcinoma [Yanagawa et al., 1999; Yanagawa et al., 2000; Chang et al., 2001; Qi et al., 2005]. As the hypoxic and unstable oxygenation microenvironment of a tumor is one of the key factors influencing tumor growth and progression, the induction of Prx1 expression might be an adaptive response of the cancer cells [Zhang et al., 2009]. Although the molecular mechanism responsible for the abnormal elevation of Prx1 is still unclear, it may be interesting to investigate the gene polymorphisms of E6AP and the stability of Prx1 in cancer cells.

There are several modes of substrate recognition in the ubiquitin–proteasome system. Recognition can be made via several mechanisms, such as (1) NH_2-terminal residues (the N-end rule pathway), (2) allosteric activation, (3) recognition of phosphorylated substrate, (4) phosphorylation of E3, (5) phosphorylation of both the ligase and its substrate, (6) recognition in trans via an ancillary protein, (7) abnormal/mutated/misfolded proteins, and (8) recognition via hydroxylated protein [Glickman and Ciechanover, 2002]. It is known that E6AP uses several mechanisms for substrate recognition. E6AP recognizes p53 in conjunction with the HPV16 E6 protein [Scheffner et al., 1993; Talis et al., 1998]. E6AP also recognizes the tyrosine-phosphorylated form of Blk [Oda et al., 1999] and the Ca^{2+}-binding form of annexin A1 [Shimoji et al., 2009]. Further studies will be needed to elucidate the mode of Prx1 recognition by E6AP.

In conclusion, we demonstrated that E6AP mediates the ubiquitin-dependent degradation of Prx1. Future efforts will focus on understanding the role of the E6AP-mediated proteolysis of Prx1 in the defense against oxidative stress and thermal stress as well as the ubiquitylation signal of Prx1. Insights into the physiological function of E6AP will be gained by investigating the effects of various oxidative stresses on the stability and functional control of Prx1.

ACKNOWLEDGMENTS

We thank Dr. Bohmann (EMBL) for providing pMT123 and Dr. Iwai (Osaka University) for recombinant baculovirus carrying His_6-mouse E1. We also thank T. Mizoguchi and K. Hachida for secretarial work. This work was supported in part by a grant from the 100th Anniversary of the Foundation of the Nippon Dental University; by a grant for Research on Health Sciences focusing on Drug Innovation from the Japan Health Sciences Foundation; by grants-in-aid from the Ministry of Health, Labour, and Welfare; by a grant from the Ministry of Education, Science and Culture of Japan; by the program for Promotion of Fundamental Studies in Health Sciences of the National Institute of Biomedical Innovation (NIBIO), Japan.

REFERENCES

Chang JW, Jeon HB, Lee JH, Yoo JS, Chun JS, Kim JH, Yoo YJ. 2001. Augmented expression of peroxiredoxin I in lung cancer. Biochem Biophys Res Commun 289:507–512.

Chang TS, Jeong W, Choi SY, Yu S, Kang SW, Rhee SG. 2002. Regulation of peroxiredoxin I activity by Cdc2-mediated phosphorylation. J Biol Chem 277:25370–25376.

Cooper EM, Hudson AW, Amos J, Wagstaff J, Howley PM. 2004. Biochemical analysis of Angelman syndrome-associated mutations in the E3 ubiquitin ligase E6-associated protein. J Biol Chem 279:41208–41217.

Dan B. 2009. Angelman syndrome: Current understanding and research prospects. Epilepsia 50:2331–2339.

Gewin L, Myers H, Kiyono T, Galloway DA. 2004. Identification of a novel telomerase repressor that interacts with the human papillomavirus type-16 E6/E6-AP complex. Genes Dev 18:2269–2282.

Glickman MH, Ciechanover A. 2002. The ubiquitin-proteasome proteolytic pathway: Destruction for the sake of construction. Physiol Rev 82:373–428.

Hall A, Karplus PA, Poole LB. 2009. Typical 2-Cys peroxiredoxins—Structures, mechanisms and functions. FEBS J 276:2469–2477.

Huibregtse JM, Scheffner M, Howley PM. 1993. Cloning and expression of the cDNA for E6-AP, a protein that mediates the interaction of the human papillomavirus E6 oncoprotein with p53. Mol Cell Biol 13:775–784.

Huibregtse JM, Scheffner M, Beaudenon S, Howley PM. 1995. A family of proteins structurally and functionally related to the E6-AP ubiquitin-protein ligase. Proc Natl Acad Sci USA 92:2563–2567.

Ichimura T, Yamamura H, Sasamoto K, Tominaga Y, Taoka M, Kakiuchi K, Shinkawa T, Takahashi N, Shimada S, Isobe T. 2005. 14-3-3 proteins modulate the expression of epithelial Na+ channels by phosphorylation-dependent interaction with Nedd 4-2 ubiquitin ligase. J Biol Chem 280: 13187–13194.

Immenschuh S, Iwahara S, Schwennen B. 2002. Induction of heme-binding protein 23/peroxiredoxin I gene expression by okadaic acid in cultured rat hepatocytes. DNA Cell Biol 21:347–354.

Jang HH, Lee KO, Chi YH, Jung BG, Park SK, Park JH, Lee JR, Lee SS, Moon JC, Yun JW, Choi YO, Kim WY, Kang JS, Cheong GW, Yun DJ, Rhee SG, Cho MJ, Lee SY. 2004. Two enzymes in one; Two yeast peroxiredoxins display oxidative stress-dependent switching from a peroxidase to a molecular chaperone function. Cell 117:625–635.

Kang SW, Baines IC, Rhee SG. 1998. Characterization of a mammalian peroxiredoxin that contains one conserved cysteine. J Biol Chem 273: 6303–6311.

Kishino T, Lalande M, Wagstaff J. 1997. UBE3A/E6-AP mutations cause Angelman syndrome. Nat Genet 15:70–73.

Kuhne C, Banks L. 1998. E3-ubiquitin ligase/E6-AP links multicopy maintenance protein 7 to the ubiquitination pathway by a novel motif, the L2G box. J Biol Chem 273:34302–34309.

Kumar S, Talis AL, Howley PM. 1999. Identification of HHR23A as a substrate for E6-associated protein-mediated ubiquitination. J Biol Chem 274:18785–18792.

Lim KL, Chew KC, Tan JM, Wang C, Chung KK, Zhang Y, Tanaka Y, Smith W, Engelender S, Ross CA, Dawson VL, Dawson TM. 2005. Parkin mediates nonclassical, proteasomal-independent ubiquitination of synphilin-1: Implications for Lewy body formation. J Neurosci 25:2002–2009.

Mani A, Oh AS, Bowden ET, Lahusen T, Lorick KL, Weissman AM, Schlegel R, Wellstein A, Riegel AT. 2006. E6AP mediates regulated proteasomal degradation of the nuclear receptor coactivator amplified in breast cancer 1 in immortalized cells. Cancer Res 66:8680–8686.

Matentzoglu K, Scheffner M. 2008. Ubiquitin ligase E6-AP and its role in human disease. Biochem Soc Trans 36:797–801.

Matsuura T, Sutcliffe JS, Fang P, Galjaard RJ, Jiang YH, Benton CS, Rommens JM, Beaudet AL. 1997. De novo truncating mutations in E6-AP ubiquitin-protein ligase gene (UBE3A) in Angelman syndrome. Nat Genet 15:74–77.

Nakagawa S, Huibregtse JM. 2000. Human scribble (Vartul) is targeted for ubiquitin-mediated degradation by the high-risk papillomavirus E6 proteins and the E6AP ubiquitin-protein ligase. Mol Cell Biol 20:8244–8253.

Natsume T, Yamauchi Y, Nakayama H, Shinkawa T, Yanagida M, Takahashi N, Isobe T. 2002. A direct nanoflow liquid chromatography-tandem mass spectrometry system for interaction proteomics. Anal Chem 74:4725–4733.

Oda H, Kumar S, Howley PM. 1999. Regulation of the Src family tyrosine kinase Blk through E6AP-mediated ubiquitination. Proc Natl Acad Sci USA 96:9557–9562.

Qi Y, Chiu JF, Wang L, Kwong DL, He QY. 2005. Comparative proteomic analysis of esophageal squamous cell carcinoma. Proteomics 5:2960–2971.

Rhee SG, Chae HZ, Kim K. 2005. Peroxiredoxins: A historical overview and speculative preview of novel mechanisms and emerging concepts in cell signaling. Free Radic Biol Med 38:1543–1552.

Scheffner M, Huibregtse JM, Vierstra RD, Howley PM. 1993. The HPV-16 E6 and E6-AP complex functions as a ubiquitin-protein ligase in the ubiquitination of p53. Cell 75:495–505.

Scheffner M, Huibregtse JM, Howley PM. 1994. Identification of a human ubiquitin-conjugating enzyme that mediates the E6-AP-dependent ubiquitination of p53. Proc Natl Acad Sci USA 91:8797–8801.

Shimoji T, Murakami K, Sugiyama Y, Matsuda M, Inubushi S, Nasu J, Shirakura M, Suzuki T, Wakita T, Kishino T, Hotta H, Miyamura T, Shoji I. 2009. Identification of annexin A1 as a novel substrate for E6AP-mediated ubiquitylation. J Cell Biochem 106:1123–1135.

Shirakura M, Murakami K, Ichimura T, Suzuki R, Shimoji T, Fukuda K, Abe K, Sato S, Fukasawa M, Yamakawa Y, Nishijima M, Moriishi K, Matsuura Y, Wakita T, Suzuki T, Howley PM, Miyamura T, Shoji I. 2007. E6AP ubiquitin ligase mediates ubiquitylation and degradation of hepatitis C virus core protein. J Virol 81:1174–1185.

Suzuki R, Moriishi K, Fukuda K, Shirakura M, Ishii K, Shoji I, Wakita T, Miyamura T, Matsuura Y, Suzuki T. 2009. Proteasomal turnover of hepatitis C virus core protein is regulated by two distinct mechanisms: A ubiquitin-dependent mechanism and a ubiquitin-independent but PA28gamma-dependent mechanism. J Virol 83:2389–2392.

Talis AL, Huibregtse JM, Howley PM. 1998. The role of E6AP in the regulation of p53 protein levels in human papillomavirus (HPV)-positive and HPV-negative cells. J Biol Chem 273:6439–6445.

Wijayanti N, Naidu S, Kietzmann T, Immenschuh S. 2008. Inhibition of phorbol ester-dependent peroxiredoxin I gene activation by lipopolysaccharide via phosphorylation of RelA/p65 at serine 276 in monocytes. Free Radic Biol Med 44:699–710.

Woo HA, Chae HZ, Hwang SC, Yang KS, Kang SW, Kim K, Rhee SG. 2003. Reversing the inactivation of peroxiredoxins caused by cysteine sulfinic acid formation. Science 300:653–656.

Wood ZA, Poole LB, Karplus PA. 2003a. Peroxiredoxin evolution and the regulation of hydrogen peroxide signaling. Science 300:650–653.

Wood ZA, Schroder E, Robin Harris J, Poole LB. 2003b. Structure, mechanism and regulation of peroxiredoxins. Trends Biochem Sci 28:32–40.

Yan Y, Sabharwal P, Rao M, Sockanathan S. 2009. The antioxidant enzyme Prdx1 controls neuronal differentiation by thiol-redox-dependent activation of GDE2. Cell 138:1209–1221.

Yanagawa T, Ishikawa T, Ishii T, Tabuchi K, Iwasa S, Bannai S, Omura K, Suzuki H, Yoshida H. 1999. Peroxiredoxin I expression in human thyroid tumors. Cancer Lett 145:127–132.

Yanagawa T, Iwasa S, Ishii T, Tabuchi K, Yusa H, Onizawa K, Omura K, Harada H, Suzuki H, Yoshida H. 2000. Peroxiredoxin I expression in oral cancer: A potential new tumor marker. Cancer Lett 156:27–35.

Yang Y, Liu W, Zou W, Wang H, Zong H, Jiang J, Wang Y, Gu J. 2007. Ubiquitin-dependent proteolysis of trihydrophobin 1 (TH1) by the human papilloma virus E6-associated protein (E6-AP). J Cell Biochem 101:167–180.

Zhang B, Wang Y, Su Y. 2009. Peroxiredoxins, a novel target in cancer radiotherapy. Cancer Lett 286:154–160.

JOURNAL OF VIROLOGY, Sept. 2011, p. 8556–8568 Vol. 85, No. 17
0022-538X/11/$12.00 doi:10.1128/JVI.00146-11

Hepatitis C Virus Infection Promotes Hepatic Gluconeogenesis through an NS5A-Mediated, FoxO1-Dependent Pathway▽

Lin Deng,[1] Ikuo Shoji,[1] Wataru Ogawa,[2] Shusaku Kaneda,[1] Tomoyoshi Soga,[3] Da-peng Jiang,[1] Yoshi-Hiro Ide,[1] and Hak Hotta[1]*

Division of Microbiology, Center for Infectious Diseases,[1] and Division of Diabetes, Metabolism and Endocrinology,[2] Kobe University Graduate School of Medicine, 7-5-1 Kusunoki-cho, Chuo-ku, Kobe 650-0017, Japan, and Institute for Advanced Biosciences, Keio University, 246-2 Mizukami, Kakuganji, Tsuruoka, Yamagata 997-0052, Japan[3]

Received 21 January 2011/Accepted 7 June 2011

Chronic hepatitis C virus (HCV) infection is often associated with type 2 diabetes. However, the precise mechanism underlying this association is still unclear. Here, using Huh-7.5 cells either harboring HCV-1b RNA replicons or infected with HCV-2a, we showed that HCV transcriptionally upregulated the genes for phosphoenolpyruvate carboxykinase (PEPCK) and glucose 6-phosphatase (G6Pase), the rate-limiting enzymes for hepatic gluconeogenesis. In this way, HCV enhanced the cellular production of glucose 6-phosphate (G6P) and glucose. PEPCK and G6Pase gene expressions are controlled by the transcription factor forkhead box O1 (FoxO1). We observed that although neither the mRNA levels nor the protein levels of FoxO1 expression were affected by HCV, the level of phosphorylation of FoxO1 at Ser319 was markedly diminished in HCV-infected cells compared to the control cells, resulting in an increased nuclear accumulation of FoxO1, which is essential for sustaining its transcriptional activity. It was unlikely that the decreased level of FoxO1 phosphorylation was mediated through Akt inactivation, as we observed an increased phosphorylation of Akt at Ser473 in HCV-infected cells compared to control cells. By using specific inhibitors of c-Jun N-terminal kinase (JNK) and reactive oxygen species (ROS), we demonstrated that HCV infection induced JNK activation via increased mitochondrial ROS production, resulting in decreased FoxO1 phosphorylation, FoxO1 nuclear accumulation, and, eventually, increased glucose production. We also found that HCV NS5A mediated increased ROS production and JNK activation, which is directly linked with the FoxO1-dependent increased gluconeogenesis. Taken together, these observations suggest that HCV promotes hepatic gluconeogenesis through an NS5A-mediated, FoxO1-dependent pathway.

Hepatitis C virus (HCV) is a small, enveloped RNA virus that belongs to the genus *Hepacivirus* of the family *Flaviviridae*, and the molecular mechanisms underlying its viral replication are currently being unraveled (40). The HCV genome encodes a single polyprotein of about 3,000 amino acids, which is cleaved by host and viral proteases to generate at least 10 viral proteins, such as core, envelope 1 (E1), E2, p7, NS2, NS3, NS4A, NS4B, NS5A, and NS5B. HCV can be classified into seven genotypes, with each genotype further classified into a number of subtypes, such as HCV-1a and HCV-1b (18, 24, 59).

HCV infects more than 120 million people worldwide (57). Persistent HCV infection causes not only liver diseases (chronic hepatitis, liver cirrhosis, and hepatocellular carcinoma) but also extrahepatic manifestations, such as type 2 diabetes (2, 11, 20, 23). While it is known that liver cirrhosis impairs the glucose metabolism of the liver, there are some reports showing that HCV-infected patients over 40 years of age have an increased risk of type 2 diabetes compared with individuals without HCV infection (43). In addition, insulin receptor substrate 1 (IRS-1)/phosphatidylinositol 3-kinase (PI3-kinase) signaling was more impaired in HCV-infected patients than in non-HCV-infected controls (3). These studies imply that HCV infection may directly predispose the host toward type 2 diabetes. However, the precise mechanisms are poorly understood.

Hepatocytes play an important role in maintaining plasma glucose homeostasis by adjusting the balance between hepatic glucose production and utilization via the gluconeogenic and glycolytic pathways, respectively. It was proposed previously that increased hepatic glucose production is a major feature of type 2 diabetes (13). It is also known that hyperglycemia and the subsequent development of type 2 diabetes mellitus result, at least in part, from impaired insulin signaling together with elevated glucagon levels (5, 19). Hepatic glucose production and utilization, physiologically opposed cascades, are regulated, at least in part, at the transcriptional level of the glucose 6-phosphatase (G6Pase) and glucokinase (GK) genes, which catalyze the last and the first rate-limiting steps in gluconeogenesis and glycolysis, respectively. A number of studies have shown that fasting/feeding (or hormones) controls the transcription of these two enzymes in the opposite directions. G6Pase transcription is negatively regulated by insulin or feeding and is markedly increased in a fasting state (62). On the other hand, GK transcription is positively regulated by insulin or feeding and markedly decreased in a fasting state (33). It has also been reported that the gene expressions of gluconeogenic and glycolytic enzymes, such as G6Pase, GK, and phosphoenolpyruvate carboxykinase (PEPCK), another rate-limiting enzyme for hepatic gluconeogenesis, are regulated by certain

* Corresponding author. Mailing address: Division of Microbiology, Center for Infectious Disease, Kobe University Graduate School of Medicine, 7-5-1 Kusunoki-cho, Chuo-ku, Kobe 650-0017, Japan. Phone: 81-78-382-5500. Fax: 81-78-382-5519. E-mail: hotta@kobe-u.ac.jp.

▽ Published ahead of print on 22 June 2011.

TABLE 1. Sequences and positions of primers used in this study

Gene (GenBank accession no.)	Primer	Positions	PCR product (bp)
GK (M69051)	5′-GCCTCCCAAAGCATCTACCTC-3′ 5′-GCTCCACTGCCCCTCCTCACC-3′	119–139 562–542	444
G6Pase (U01120)	5′-CCTGGGGCTGGCTCTCAACTC-3′ 5′-AATAGTAGTCCTCCTCAATCC-3′	889–909 1197–1177	309
PEPCK (BC023978)	5′-CCAGGCAGTGAGGGAGTTTCT-3′ 5′-ACTGTGTCTCTTTGCTCTTGG-3′	210–230 426–406	217
FoxO1 (NM_002915)	5′-GAGGGTTAGTGAGCAGGTTAC-3′ 5′-AGTCCTTATCTACAGCAGCAC-3′	2352–2372 2568–2548	217
HCV NS5A (JF343793)	5′-AGACGTATTGAGGTCCATGC-3′ 5′-CCGCAGCGACGGTGCTGATAG-3′	6899–6918 7011–7031	133
β-Glucuronidase (M15182)	5′-ATCAAAAACGCAGAAAATACG-3′ 5′-ACGCAGGTGGTATCAGTCTTG-3′	1747–1767 1984–1964	238
GAPDH (NM_002046)	5′-GCCATCAATGACCCCTTCATT-3′ 5′-TCTCGCTCCTGGAAGATGG-3′	196–216 326–344	149

transcription factors, including forkhead box O1 (FoxO1) (26, 50, 54), hepatic nuclear factor 4α (HNF-4α) (26), Krüppel-like factor 15 (KLF15) (64), and cyclic AMP (cAMP) response element binding protein (CREB) (52, 56). The deregulation of the otherwise balanced control of hepatic glucose homeostasis would potentially lead to hyperglycemia and, eventually, type 2 diabetes.

In this study, by using Huh-7.5 cells harboring HCV-1b RNA replicons, i.e., either a subgenomic RNA replicon (SGR) or a full-genomic RNA replicon (FGR) (37), and cells infected with HCV-2a (14, 37, 39), we investigated the possible effects of HCV on glucose metabolism. We report here that HCV promotes hepatic gluconeogenesis, resulting in increased cellular glucose production in hepatocytes via an NS5A-mediated, FoxO1-dependent pathway.

MATERIALS AND METHODS

Cells, HCV RNA replicons, and virus. The human hepatoma-derived cell line Huh-7.5 (7) was kindly provided by C. M. Rice (Rockefeller University, New York, NY). The SGR and FGR were prepared by using pFK5B/2884Gly (41) (a kind gift from R. Bartenschlager, University of Heidelberg, Heidelberg, Germany) and pON/C-5B (31) (a kind gift from N. Kato, Okayama University, Okayama, Japan), respectively. The SGR and FGR cells are of polyclonal origin to avoid clonal variation. Plasmid pFL-J6/JFH1, which encodes the entire viral genome of a chimeric strain of HCV-2a (J6/JFH1) (39), was kindly provided by C. M. Rice. The HCV RNA genome was transcribed *in vitro* from pFL-J6/JFH1 and transfected into Huh-7.5 cells to yield infectious HCV particles, as described previously (14). A cell culture-adapted P-47 strain (9, 14) was used throughout the experiments. Virus infection was performed at a multiplicity of infection (MOI) of 2.0. Virus infectivity was measured by indirect immunofluorescence analysis, as described below, and expressed as cell-infecting units/ml. In some experiments, SGR and FGR cells, as well as HCV-infected cells at 5 days after virus infection, were treated with 1,000 IU/ml of alpha interferon (IFN) (Sigma Chemical, St. Louis, MO) for 10 days to eliminate HCV replication.

Plasmid construction. Expression plasmids for core, p7, NS2, NS3, NS3/4A, NS4A, NS4B, NS5A, and NS5B were reported elsewhere previously (15, 32).

Real-time quantitative RT-PCR. Total cellular RNA was isolated by using RNAiso reagent (Takara, Kyoto, Japan), and cDNA was generated by using a QuantiTect reverse transcription (RT) system (Qiagen, Valencia, CA). Real-time quantitative PCR was performed by using SYBR Premix Ex *Taq* (Takara) with SYBR green chemistry on an ABI Prism 7000 system (Applied Biosystems, Foster City, CA), as reported previously (37). β-Glucuronidase and GAPDH (glyceraldehyde-3-phosphate dehydrogenase) were used as internal controls. The primers used are shown in Table 1.

G6P production assay. Huh-7.5 cells seeded into a 10-cm dish at a density of 1.0×10^6 cells/dish were infected with HCV or left uninfected. At different time points after infection, the cells were washed twice with 5% mannitol solution and covered with methanol (1 ml) containing 25 μM (each) four internal standards (3-aminopyrolidine, L-methionine sulfone, trimesate, and 2-morpholinoethanesulfonic acid) for enzyme inactivation. The mixtures of methanol and cells were collected and mixed with Milli-Q water and chloroform at ratios of 2:1:2. Both the medium and cell sample solutions were then centrifuged at 20,000 × *g* for 15 min, and the aqueous layers were collected for centrifugal filtration through a 5-kDa-cutoff filter at 9,000 × *g* for 2 h. The extracted metabolites were concentrated with a centrifugal concentrator and stored at −80°C until analysis. Glucose 6-phosphate (G6P) concentrations were measured by capillary electrophoresis time-of-flight mass spectrometry (CE-TOFMS), and the results were normalized to the cell number as described previously (60, 61).

Glucose production assay. Culture medium was replaced with glucose production buffer consisting of glucose-free Dulbecco's modified Eagle's medium (DMEM) (Sigma Chemical), without phenol red, supplemented with a gluconeogenic substrate (2 mM sodium pyruvate and 20 mM sodium lactate). After 24 h of incubation, the medium was collected, and the total glucose concentration was measured by using a commercial kit (Glucose CII Test Wako; Wako Pure Chemical Industries, Osaka, Japan) and normalized to the cellular protein content. As the baseline of glucose production, glucose-free DMEM with neither sodium pyruvate nor sodium lactate was used. Glucose production via gluconeogenesis equals the total glucose production minus the baseline glucose production.

Luciferase reporter assay. The PEPCK gene promoter (position −1263/+225) and a deletion mutant (position −998/+225) were inserted into the pGL3 luciferase reporter plasmid (Promega, Madison, WI). The constructs were designated rPEPCK-P5(−1263)-pGL3basic and rPEPCK-P4(−998)-pGL3basic. pRL-CMV-Renilla (Promega), which expresses *Renilla* luciferase, was used as an internal control. Huh-7.5 cells prepared in a 12-well tissue culture plate at a density of 1.0×10^5 cells/well were transiently transfected with pRL-CMV-Renilla and rPEPCK-P5(−1263)-pGL3basic or rPEPCK-P4(−998)-pGL3basic in the presence of pEF1/NS4A, pEF1/NS5A, or a control vector (32). After 48 h, a luciferase assay was performed by using the Dual-Luciferase reporter assay system (Promega). Firefly and *Renilla* luciferase activities were measured with a Lumat LB 9501 luminometer (Berthold, Bad Wildbad, Germany). Firefly luciferase activity was normalized to *Renilla* luciferase activity for each sample.

Detection of mitochondrial ROS. Mitochondrial reactive oxygen species (ROS) production was analyzed as described previously (14). Briefly, cells seeded onto glass coverslips in a 24-well plate were incubated with 5 μM MitoSOX red (Molecular Probes, Eugene, OR) at 37°C for 10 min and then fixed with 3.7% paraformaldehyde and observed under a confocal laser scanning microscope (Carl Zeiss, Oberkochen, Germany). When needed, the fixed cells

were subjected to indirect immunofluorescence analysis to confirm HCV infection or NS5A expression, as described below.

Indirect immunofluorescence. Huh-7.5 cells seeded onto glass coverslips in a 24-well plate were infected with HCV or transfected with an NS5A expression plasmid. At 5 days postinfection (dpi) or 3 days posttransfection, the cells were fixed with 3.7% paraformaldehyde in phosphate-buffered saline (PBS) for 15 min at room temperature and permeabilized with 0.1% Triton X-100 in PBS for 15 min at room temperature. Mock-infected or empty-vector-transfected cells were similarly treated as controls for comparisons. After being washed with PBS twice, cells were consecutively stained with primary and secondary antibodies. The primary antibodies used were anti-FoxO1 rabbit monoclonal antibody (Cell Signaling Technology, Danvers, MA), anti-NS5A mouse monoclonal antibody (Chemicon International, Temecula, CA), and serum from an HCV-infected patient. Secondary antibodies used were Alexa Fluor 488-conjugated goat anti-rabbit immunoglobulin G (IgG), Alexa Fluor 594-conjugated goat anti-mouse IgG or anti-human IgG (Molecular Probes), and fluorescein isothiocyanate (FITC)-conjugated goat anti-mouse IgG or anti-human IgG (MBL, Nagoya, Japan). The stained cells were observed under a confocal laser scanning microscope (Carl Zeiss).

Cell fractionation and immunoblotting. Nuclear and cytoplasmic extracts from cells were prepared by using an NE-PER nuclear and cytoplasmic extraction reagent kit (Pierce Chemical, Rockford, IL). For immunoblotting, cells were lysed with SDS sample buffer, and equal amounts of protein were subjected to SDS-polyacrylamide gel electrophoresis and transferred onto a polyvinylidene difluoride membrane (Millipore, Bedford, MA), which was then incubated with the respective primary antibodies. The primary antibodies used were mouse monoclonal antibodies against HCV core (clone 2H9; a kind gift from T. Wakita, Department of Virology II, National Institute of Infectious Diseases, Tokyo, Japan), NS3, NS4A, NS5A, GAPDH (Chemicon), FoxO1 (Sigma Chemical), phospho-Akt (Ser473) (Cell Signaling Technology), and c-Myc (9E10; Santa Cruz Biotechnology, Santa Cruz, CA); rabbit polyclonal antibodies against phospho-FoxO1 (Ser139), Oct-1 (Santa Cruz Biotechnology), c-Jun N-terminal kinase (JNK), phospho-JNK (Thr183/Tyr185), c-Jun, phospho-c-Jun (Ser63), and Akt (Cell Signaling Technology); and goat polyclonal antibody against HSP60 (Santa Cruz Biotechnology). Horseradish peroxidase-conjugated goat anti-mouse IgG, goat anti-rabbit IgG (Molecular Probes), and donkey anti-goat IgG (Santa Cruz Biotechnology) were used to visualize the respective proteins by means of an enhanced chemiluminescence detection system (ECL; GE Healthcare, Buckinghamshire, United Kingdom).

Statistical analysis. Results were expressed as means ± standard errors of the means (SEM). Statistical significance was evaluated by analysis of variance (ANOVA) and was defined as a P value of <0.05.

RESULTS

HCV upregulates gene expression of PEPCK and G6Pase and downregulates gene expression of GK. We first examined the expression levels of the genes for the rate-limiting enzymes in hepatic gluconeogenesis, PEPCK and G6Pase, and of those for GK, which catalyzes the first step of glycolysis, by means of real-time quantitative RT-PCR analysis. We observed that the PEPCK and G6Pase genes were transcriptionally activated in SGR- and FGR-harboring cells (Fig. 1A and B, left). Similarly, the PEPCK and G6Pase genes were upregulated in HCV-infected cells in a time-dependent manner, starting from 3 or 5 days postinfection (dpi) up to 14 dpi (Fig. 1A and B, middle). On the other hand, the GK gene was transcriptionally downregulated in SGR- and FGR-harboring cells and HCV-infected cells in a time-dependent manner (Fig. 1C). It is noteworthy that the gene expressions of six glycolytic enzymes (not including GK) were observed to be upregulated in HCV-infected cells at 1 dpi (16).

When IFN treatment eliminated HCV from the cells, the observed upregulation of PEPCK and G6Pase gene expressions as well as the downregulation of GK gene expression in SGR- and FGR-harboring cells and HCV-infected cells were cancelled (Fig. 1A, B, and C, left and right). Thus, our results suggest that there was a trend toward an increase in gluconeogenesis in SGR- and FGR-harboring cells and HCV-infected cells. In subsequent studies we further examined whether or not HCV replication was correlated with gluconeogenesis.

HCV promotes cellular production of glucose and G6P. We then examined the effect of HCV on cellular glucose production. The results showed that SGR- and FGR-harboring cells and HCV-infected cells produced greater amounts of glucose than did the control cells (Fig. 2A, top and middle). IFN treatment cancelled the enhanced glucose production in SGR- and FGR-harboring cells and in HCV-infected cells (Fig. 2A, top and bottom). We also investigated the production of G6P, which is an important precursor molecule that is converted to glucose in the gluconeogenesis pathway, by means of metabolome analysis. As shown in Fig. 2B, a significantly higher level of G6P was accumulated in HCV-infected cells than in control cells. Taken together, these results indicate that HCV indeed promotes hepatic gluconeogenesis to cause hyperglycemia. In the following analyses, we examined the possible mechanisms of HCV-induced increased gluconeogenesis.

HCV suppresses FoxO1 phosphorylation at Ser319, leading to the nuclear accumulation of FoxO1. It was demonstrated previously that FoxO1 in hepatocytes enhances gluconeogenesis through the transcriptional activation of various genes, including G6Pase and PEPCK (25). To investigate the possible effects of FoxO1 on HCV-induced gluconeogenesis, we examined the gene expression levels of FoxO1 by real-time quantitative RT-PCR analysis. As shown in Fig. 3A, there was neither an upregulation nor a downregulation of FoxO1 gene expression in SGR- or FGR-harboring cells or HCV-infected cells. The FoxO1 transcription factor is controlled by various post-translational modifications, which include phosphorylation, ubiquitylation, and acetylation. The phosphorylated form of FoxO1 is exported from the nucleus and thereby loses its transcriptional function (30). We therefore examined the phosphorylation status of FoxO1 at Ser319, which is critical for FoxO1 nuclear exclusion (72). The results showed that FoxO1 phosphorylation at Ser319 was markedly suppressed in HCV-infected cells from 4 dpi up to 8 dpi, compared to that in the HCV-negative control cells (Fig. 3B, first panel), in a time-dependent manner that was roughly the inverse of the pattern observed for PEPCK and G6Pase mRNA upregulations (Fig. 1A and B) and glucose production (Fig. 2A), while the total protein expression levels of FoxO1 were unchanged (Fig. 3B, second panel). Regarding this connection, Banerjee et al. reported previously that FoxO1 phosphorylation at Ser256 was also inhibited in HCV-infected cells (4). Since FoxO1 is known to be phosphorylated by Akt so as to be exported from the nucleus and transcriptionally inactivated (38), we examined whether Akt function was suppressed through its impaired phosphorylation in HCV-infected cells. The result obtained revealed that this was not the case: Akt phosphorylation was enhanced in HCV-infected cells from 4 dpi up to 6 dpi compared with the control cells (Fig. 3B, third panel), while the total protein expression levels of Akt were comparable (Fig. 3B, fourth panel). This result is consistent with a recent observation by Burdette et al. (10) showing that the Akt phosphorylation level was elevated in HCV-infected cells. These data suggest that the observed decrease in FoxO1 phosphorylation

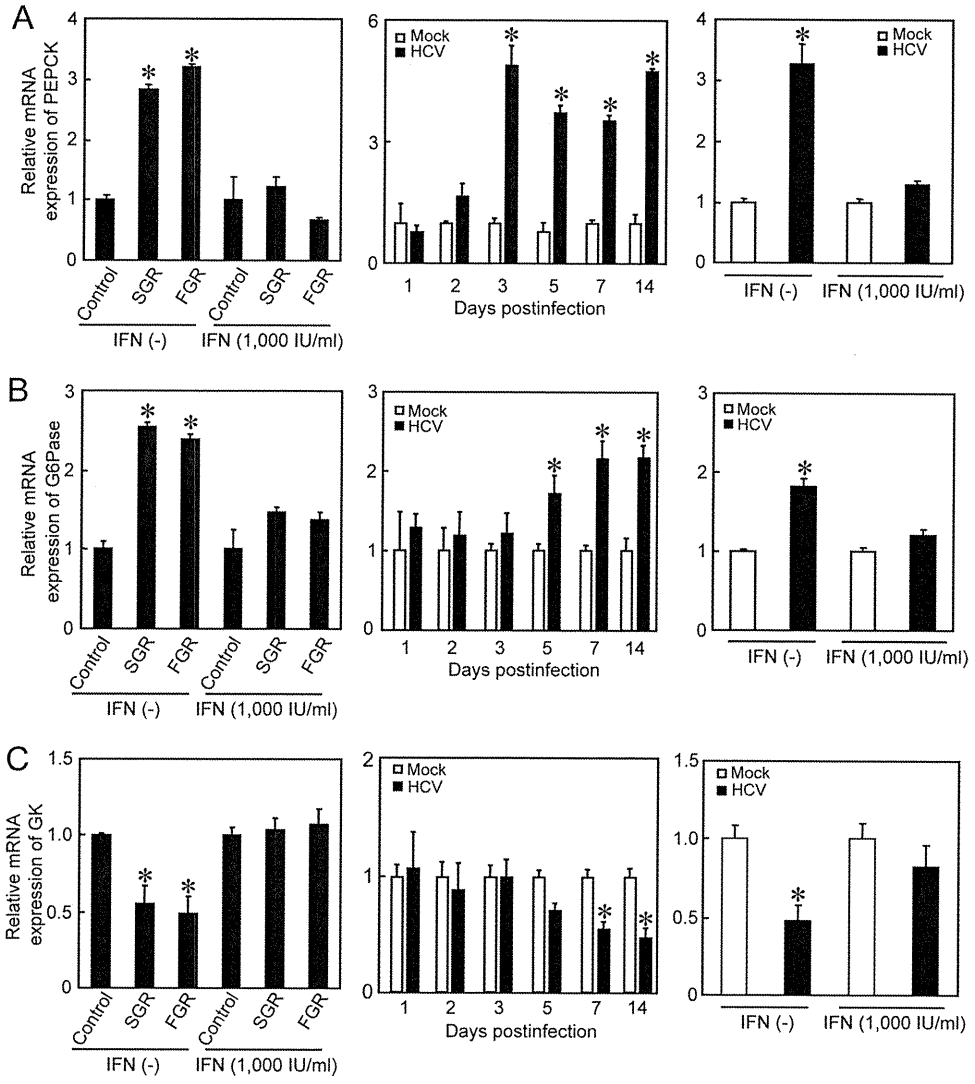

FIG. 1. HCV upregulates gene expressions of PEPCK and G6Pase and downregulates gene expression of GK. Quantitative RT-PCR analysis was performed to quantify PEPCK (A), G6Pase (B), and GK (C) mRNA expression levels in SGR- and FGR-harboring cells and HCV-infected cells (MOI = 2), and the results were normalized to β-glucuronidase mRNA expression levels. In parallel, SGR- and FGR-harboring cells and HCV-infected cells (at 5 dpi) were treated with IFN (1,000 IU/ml) for 10 days to eliminate HCV replication before being subjected to quantitative RT-PCR. Data represent means ± SEM of data from three independent experiments, and the values for the control cells were arbitrarily expressed as 1.0. *, $P < 0.01$ compared with the control.

in HCV-infected cells is caused by a mechanism independent of Akt.

Next, we tested whether HCV indeed promoted FoxO1 nuclear accumulation. The majority of FoxO1 was accumulated in the nuclear fraction in HCV-infected cells (Fig. 3C, second panel, lanes 2 and 4), whereas in control cells FoxO1 was distributed in both the nuclear and cytoplasmic fractions (lanes 1 and 3). Taken together, these results suggest that HCV suppressed FoxO1 phosphorylation, leading to the nuclear accumulation of FoxO1.

HCV-induced JNK activation is involved in the suppression of FoxO1 phosphorylation. Recent studies demonstrated that a signaling pathway that involves the stress-sensitive serine/threonine kinase JNK regulates FoxO at multiple levels (36, 66). We therefore investigated whether HCV induced JNK activation in Huh-7.5 cells. As shown in Fig. 4A, the amount of phosphorylated (activated) JNK markedly increased in HCV-infected cells in a time-dependent manner, similar to that observed for the suppression of FoxO1 phosphorylation, while the total expression levels of JNK were unchanged. As a result, c-Jun, a key substrate for JNK, was phosphorylated (activated) in HCV-infected cells but not in the mock-infected control cells. It should also be noted that the total expression levels of c-Jun in HCV-infected cells were significantly higher than those in the mock-infected control cells, suggesting that c-Jun activation through its phosphorylation stabilizes c-Jun protein expression in HCV-infected cells, as was proposed previously by Zhang et al (71).

We next sought to determine whether JNK activation was involved in the HCV-induced suppression of FoxO1 phosphorylation. HCV-infected cells at 5 days after virus infection were treated with the specific JNK inhibitor SP600125 (20 μM) (6)

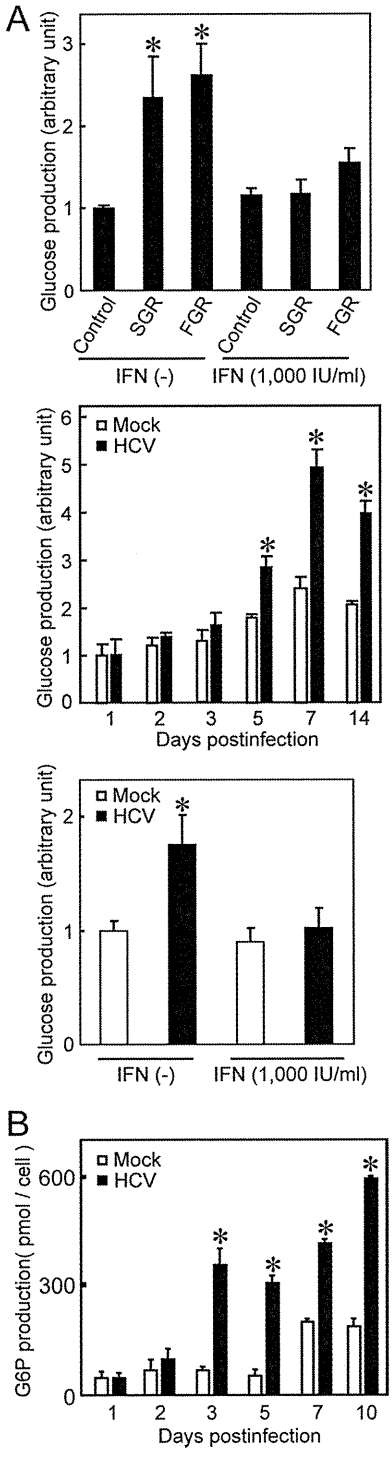

FIG. 2. HCV promotes the production of glucose and G6P. (A) Extracellular glucose production was measured in SGR- and FGR-harboring cells and HCV-infected cells (MOI = 2) and normalized to total cellular protein expression levels. In parallel, SGR- and FGR-harboring cells and HCV-infected cells (at 5 dpi) were treated with IFN (1,000 IU/ml) for 10 days to eliminate HCV replication before being subjected to glucose production analysis. Data represent means ± SEM of data from three independent experiments, and the value for the control cells was arbitrarily expressed as 1.0. *, $P < 0.01$ compared with the control. (B) Cellular G6Pase production was measured in HCV-infected cells (MOI = 2), and the results were normalized to cell numbers. Data represent means ± SEM of data from three independent experiments. *, $P < 0.01$ compared with the control.

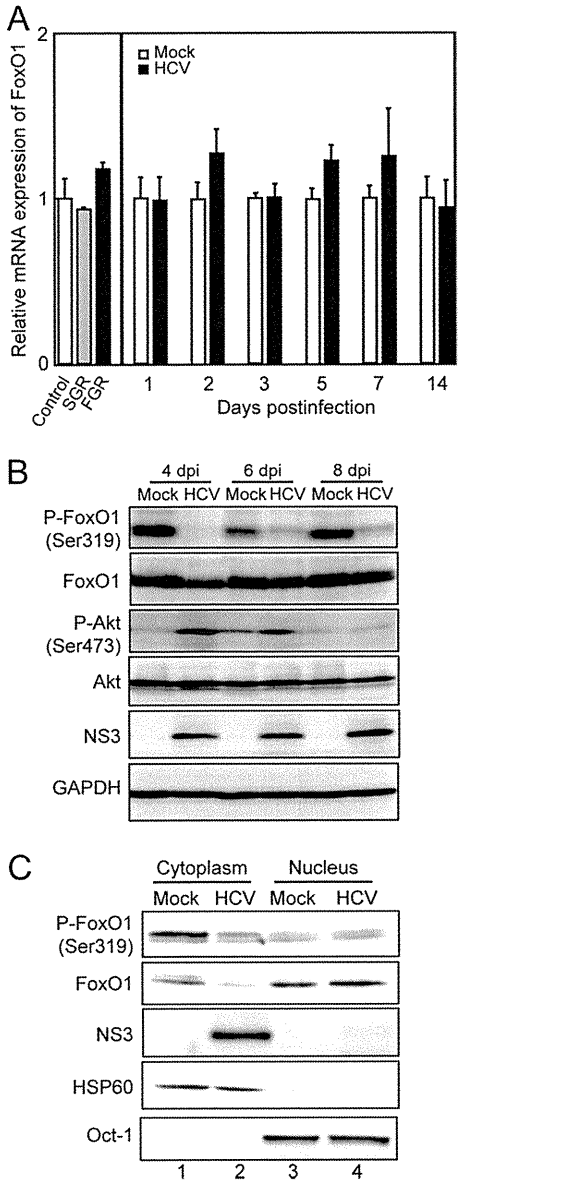

FIG. 3. HCV suppresses FoxO1 phosphorylation, leading to nuclear accumulation of FoxO1. (A) Quantitative RT-PCR analysis was performed to determine FoxO1 mRNA expression levels in SGR- and FGR-harboring cells and HCV-infected cells (MOI = 2), and expression levels were normalized to β-glucuronidase mRNA expression levels. (B) The expression levels of FoxO1, phospho-FoxO1 (Ser319) (P-FoxO1), Akt, and phospho-Akt (Ser473) were analyzed by immunoblotting of HCV-infected cells and mock-infected control cells. Blots were reprobed with antibodies recognizing NS3 and GAPDH. The amounts of GAPDH were measured as an internal control to verify equal amounts of sample loading. (C) Cytoplasmic and nuclear fractions were prepared from HCV-infected cells and mock-infected control cells at 4 dpi and were analyzed by immunoblotting using antibodies against FoxO1, phospho-FoxO1 (Ser319), NS3, Hsp60, and Oct-1. The amounts of Hsp60 and Oct-1 were measured to verify that they were equal to the amounts of cytoplasmic and nuclear fractions, respectively.

for 24 h. The catalytic JNK activity was assayed by monitoring the phosphorylation of c-Jun. As shown in Fig. 4B, SP600125 clearly prevented the phosphorylation of c-Jun and concomitantly recovered the suppression of FoxO1 phosphorylation in

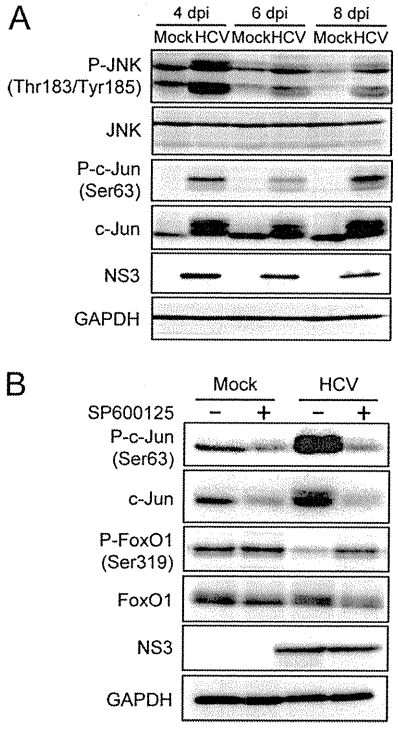

FIG. 4. HCV-induced JNK activation is required for the suppression of FoxO1 phosphorylation. (A) HCV activates the JNK/c-Jun signaling pathway. The activation (phosphorylation) of JNK (Thr183/Tyr185) and c-Jun (Ser63) in whole-cell lysates of HCV-infected cells and mock-infected control cells was analyzed by immunoblotting. Blots were reprobed with antibodies recognizing total JNK and c-Jun, NS3, and GAPDH. The amounts of GAPDH were measured as an internal control to verify equal amounts of sample loading. (B) Pretreatment with the JNK inhibitor SP600125 abrogates HCV-induced c-Jun activation and FoxO1 phosphorylation suppression. The phosphorylation of c-Jun (Ser63) and that of FoxO1 (Ser319) were analyzed by immunoblotting at 6 dpi in HCV-infected cells and mock-infected control cells with or without SP600125 pretreatment (20 μM for 24 h). Blots were reprobed with antibodies recognizing total c-Jun and FoxO1, NS3, and GAPDH. The amounts of GAPDH were measured as an internal control to verify equal amounts of sample loading.

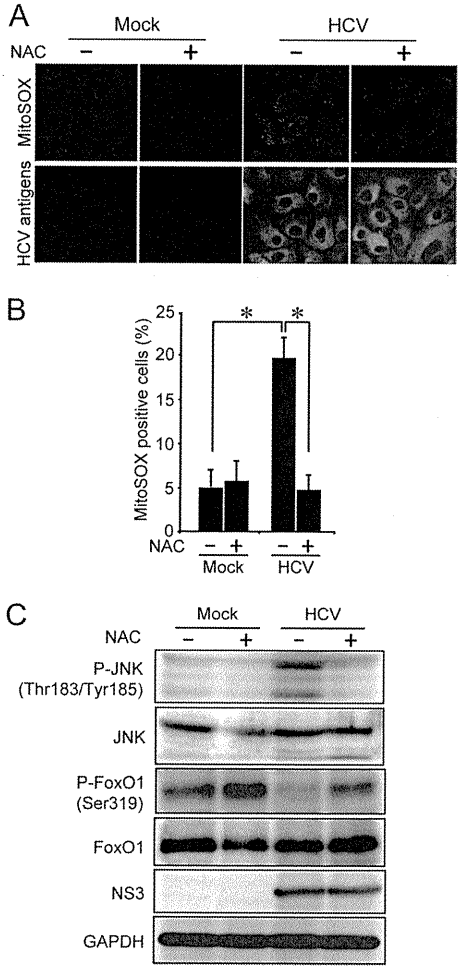

FIG. 5. HCV-induced production of mitochondrial ROS suppresses FoxO1 phosphorylation through activation of JNK. (A) Pretreatment with NAC abrogates the HCV-induced increased production of mitochondrial ROS. HCV-infected cells and mock-infected controls were pretreated with 5 mM NAC for 2 h at 6 dpi. The cells were then incubated with MitoSOX (top) and then stained for HCV antigens by using serum from an HCV-infected patient, followed by FITC-conjugated goat anti-human IgG (bottom). (B) Quantification of MitoSOX-stained cells. The percentages of cells stained with MitoSOX were determined for HCV-infected cells and mock-infected controls with or without NAC pretreatment. Data represent means ± SEM of data from two independent experiments. *, $P < 0.01$. (C) NAC pretreatment abrogates HCV-induced JNK activation and FoxO1 phosphorylation suppression. The phosphorylation of JNK (Thr183/Tyr185) and that of FoxO1 (Ser319) were analyzed by immunoblotting at 6 dpi in HCV-infected cells and mock-infected controls with or without NAC pretreatment (5 mM for 2 h). The blots were reprobed with antibodies recognizing total JNK and FoxO1, NS3, and GAPDH. The amounts of GAPDH were measured as an internal control to verify equal amounts of sample loading.

HCV-infected cells. These results suggest that HCV activates the JNK/c-Jun signaling pathway, which induces the nuclear accumulation of FoxO1 by reducing its phosphorylation status.

HCV-induced mitochondrial ROS production is involved in FoxO1 phosphorylation suppression, FoxO1 nuclear accumulation, and increased glucose production through JNK activation. We previously reported that HCV infection increases mitochondrial ROS production (14). JNK is known to be activated by ROS (35). We therefore sought to determine whether the HCV-induced increase in ROS production is an event occurring upstream of JNK activation by HCV. The pretreatment of HCV-infected cells (at 6 dpi) with 5 mM *N*-acetyl cysteine (NAC) (a general antioxidant) for 2 h significantly reduced the HCV-induced increase in ROS levels (Fig. 5A and B), as revealed by using MitoSOX, a fluorescent probe specific for superoxide that selectively accumulates in the mitochondrial compartment. As shown in Fig. 5C, NAC clearly prevented the phosphorylation of JNK and concomitantly recovered the suppression of FoxO1 phosphorylation in HCV-infected cells. These results suggest that HCV-induced ROS production is involved in JNK activation, which results in the inhibition of FoxO1 phosphorylation.

We next investigated the effects of JNK activation and ROS production on the subcellular localization of FoxO1 in HCV-infected cells by indirect immunofluorescence staining. As shown in Fig. 6A and B, FoxO1 was localized predominantly in the cytoplasm of mock-infected control cells. On the other